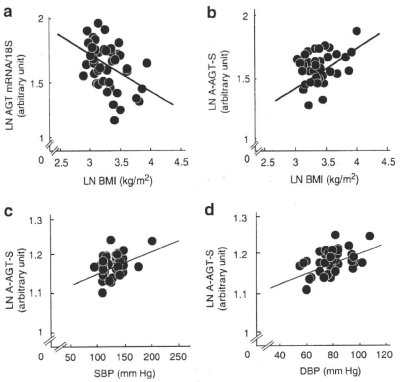


**Figure 1** | Impact of adipose tissue–derived AGT secretion on obesity and blood pressure in humans. (**a**) Relation between AGT mRNA level and BMI ($n = 46$). (**b**) Relationship between adipose tissue–derived AGT secretion (A-AGT-S) and BMI ($n = 39$). (**c**) Relationship between A-AGT-S and systolic blood pressure (SBP) ($n = 39$). (**d**) Relationship between A-AGT-S and diastolic blood pressure (DBP) ($n = 39$). AGT, angiotensinogen; BMI, body mass index; LN, natural logarithm.

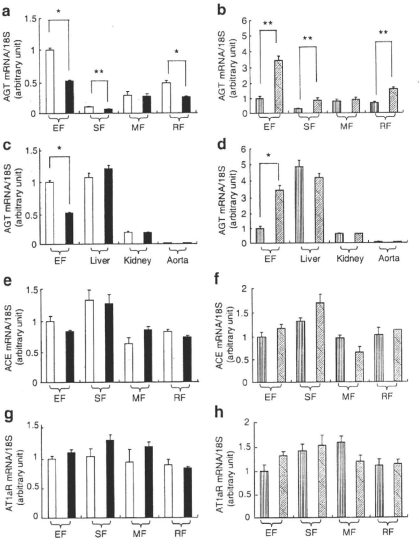


**Figure 2** | Expression of genes involved in renin–angiotensin system in obese and weight-losing mouse. AGT mRNA levels in (**a**) 12W RD ($n = 6$) and 12W DIO ($n = 6$) and in (**b**) 14W DIO ($n = 6$) and 14W WL ($n = 6$) in epididymal fat (EF), subcutaneous fat (SF), mesenteric fat (MF), and retroperitoneal fat (RF). AGT mRNA levels in (**c**) 12W RD and 12W DIO and in (**d**) 14W DIO and 14W WL in the liver, kidney, and aorta. ACE mRNA levels in (**e**) 12W RD and 12W DIO and in (**f**) 14W DIO and 14W WL. AT1aR mRNA levels in (**g**) 12W RD and 12W DIO and in (**h**) 14W DIO and 14W WL. White bar, 12W RD; black bar, 12W DIO; vertical striping bar, 14W DIO; diagonal striping bar, 14W WL. $^*P < 0.01$, $^{**}P < 0.05$. ACE, angiotensin-converting enzyme; AGT, angiotensinogen; AT1aR, angiotensin II type 1a receptor; DIO, diet-induced obesity; WL, weight-losing.

Based on the results that AGT is secreted constitutively (see **Supplementary Figure S3a–c** online), AGT mRNA expression was predicted to parallel the AGT secretion. In this context, the amount of A-AGT-S was estimated by multiplying the mRNA level of AGT/g adipose tissue with serum leptin, a representative index of body fat mass. The serum leptin level in 55 subjects was correlated with body fat mass ($r = 0.76$, $P = 0.00000000001$). Contrary to AGT mRNA level, A-AGT-S was correlated with BMI ($n = 39$, $r = 0.36$, $P = 0.02$) (**Figure 1b**). A-AGT-S was correlated with systolic blood pressure ($n = 39$, $r = 0.36$, $P = 0.02$) (**Figure 1c**) and diastolic blood pressure ($n = 39$, $r = 0.45$, $P < 0.01$) (**Figure. 1d**). In both male group ($n = 20$) and female group ($n = 19$), A-AGT-S was correlated with BMI, systolic blood pressure, and diastolic blood pressure (data not shown).

### Expression of genes involved in the RAS in obese and weight-losing mouse models

The mRNA levels of RAS genes were analyzed in obese and weight-losing mouse models described in Methods. The AGT mRNA levels in epididymal fat (EF), subcutaneous fat (SF), and retroperitoneal fat (RF) were lower in 12W DIO than in 12W RD (**Figure 2a**). In contrast, the AGT mRNA levels in EF, SF, and RF were elevated in 14W WL (**Figure 2b**). In the liver, kidney, and aorta, all of which are recognized as AGT-producing organs,[2] the AGT mRNA levels were equivalent between 12W DIO and 12W RD, or between 14W WL and 14W DIO (**Figure 2c,d**). Levels of ACE and angiotensin II type 1a receptor (AT1aR) mRNA in EF, SF, mesenteric fat (MF), and RF were also equivalent between 12W DIO and 12W RD or between 14W WL and 14W DIO (ACE: **Figure 2e,f**) (AT1aR: **Figure 2g,h**). AGT was decreased, although other genes involving RAS did not vary, in adipose tissue from the genetically obese *ob/ob* mice (data not shown).

### Adipose tissue–derived AGT secretion and plasma AGT levels in obese and weight-losing mouse models

To assess the secretion of AGT from adipose tissue in body weight change, the amounts of A-AGT-S in obese and weight-losing mice were estimated by multiplying the AGT mRNA level/g adipose tissue with the weight of EF, SF, MF, or RF. The weights of EF, SF, MF, and RF in 12W DIO were increased ~3.5-fold in comparison with 12W RD, whereas the weights of EF, SF, MF, and RF in 14W WL were decreased by one-third compared to 14W DIO. Under caloric intervention, changes in weights in the liver and kidney were subtle compared to fat depots (~20% in liver and ~5% in kidney). A-AGT-S in EF, SF, MF, and RF was significantly increased

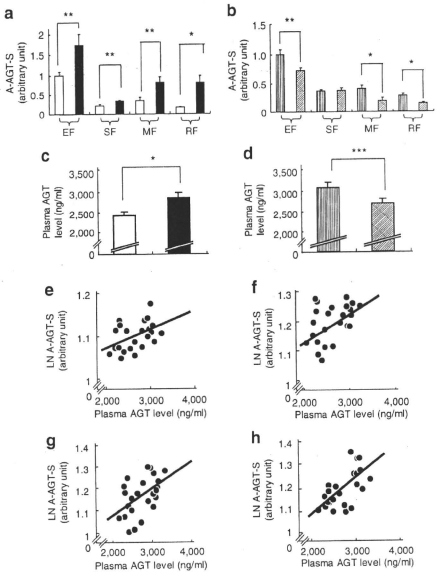


**Figure 3** | Adipose tissue–derived AGT secretion and plasma AGT level between obese and weight-losing mouse. Adipose tissue–derived AGT secretion (A-AGT-S) in (**a**) 12W RD ($n = 6$) and 12W DIO ($n = 6$) and in (**b**) 14W DIO ($n = 6$) and 14W WL ($n = 6$) in epididymal fat (EF), subcutaneous fat (SF), mesenteric fat (MF), and retroperitoneal fat (RF). Plasma AGT levels in (**c**) 12W RD and 12W DIO and in (**d**) 14W DIO and 14W WL. Relationship between A-AGT-S and plasma AGT levels in (**e**) EF, (**f**) SF, (**g**) MF, and (**h**) RF. White bar, 12W RD; black bar, 12W DIO; vertical striping bar, 14W DIO; diagonal striping bar, 14W WL. *$P < 0.01$, **$P < 0.05$, ***$P = 0.05$. AGT, angiotensinogen; DIO, diet-induced obesity; LN, natural logarithm; WL, weight-losing.

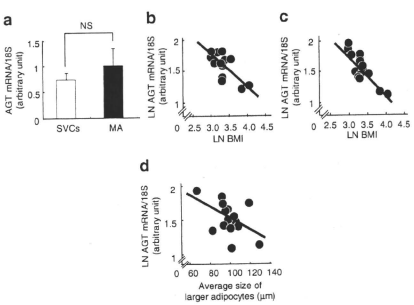


**Figure 4** | Relationship between cell size and AGT mRNA level in isolated mature adipocytes in humans. (**a**) AGT mRNA level in stromal-vascular cells (SVCs) and mature adipocytes (MAs) isolated from human subcutaneous abdominal adipose tissue (SAT) ($n = 15$; BMI: 28 ± 2.5 kg/m$^2$). White bar, SVCs; black bar, MAs. Relationship between BMI and the AGT mRNA level in (**b**) SVCs or (**c**) MAs isolated from human SAT. (**d**) Relationship between the AGT mRNA level in MAs and the average size of large adipocytes in human SAT ($n = 15$; BMI: 28 ± 2.5 kg/m$^2$). AGT, angiotensinogen; LN, natural logarithm.

in 12W DIO compared to 12W RD (**Figure 3a**). In contrast, A-AGT-S in EF, MF, and RF was decreased in 14W WL compared to 14W DIO (**Figure 3b**). To further explore the impact of obesity on circulating AGT, plasma AGT levels were measured in 12W DIO, 12W RD, 14W WL, and 14W DIO using a newly developed ELISA.[10] The plasma AGT level was elevated in 12W DIO (2,884 ± 118 ng/ml) compared to 12W RD (2,431 ± 85 ng/ml) (**Figure 3c**). In contrast, the plasma AGT level in 14W WL (2,703 ± 116 ng/ml) was lower than in 14W DIO (3,088 ± 133 ng/ml) (**Figure 3d**). A-AGT-S in EF, SF, MF, and RF were correlated with plasma AGT level in mouse of obesity and weight reduction (EF: $r = 0.49$, $P < 0.01$ (**Figure 3e**); SF: $r = 0.43$, $P = 0.02$ (**Figure 3f**); MF: $r = 0.41$, $P = 0.03$ (**Figure 3g**); RF: $r = 0.64$, $P < 0.01$ (**Figure 3h**)).

### Relationship between cell size and AGT mRNA level in isolated mature adipocytes in humans

To investigate the potential link between adipocyte size and the mRNA level of AGT in isolated MAs, adipocyte size was measured using a Coulter Multisizer[12] in human SAT ($n = 15$; BMI: 28 ± 2.5 kg/m$^2$, range: 19–55). The AGT mRNA level in MAs was comparable to that in stromal-vascular cells (**Figure 4a**).

The levels of AGT in stromal-vascular cells and MAs were inversely correlated with BMI ($r = -0.69$, $P < 0.01$ (**Figure 4b**), $r = -0.84$, $P < 0.01$ (**Figure 4c**). Consistent with a previous report,[12] the size distribution of adipocytes displayed as histograms against diameters was bimodal in all cases. The nadir was defined as the low point between the large adipocytes and small adipocytes.[12] BMI was positively correlated with both nadir size and average size of the larger adipocytes ($r = 0.50$, $P < 0.05$; $r = 0.48$, $P < 0.05$, respectively). The AGT mRNA level in isolated MA was inversely correlated with the average size of the larger adipocytes ($r = -0.48$, $P < 0.05$ (**Figure 4d**).

## DISCUSSION

The primary findings of this study are (i) A-AGT-S was substantially increased in both obese humans and obese mice. (ii) A-AGT-S was correlated with plasma AGT level in mouse models of obesity and weight reduction. A-AGT-S and plasma AGT were increased in obese mice, while decreased in mice with weight reduction. (iii) The AGT mRNA level in adipose tissue was decreased in both obese humans and mice, but increased in mice with weight reduction. The AGT mRNA levels in the liver, kidney, and aorta were not altered in mouse models of obesity and weight reduction. In contrast, expression of genes involved in RAS other than AGT did not change in adipose tissue from obese and weight-losing mice. (iv) AGT was secreted constitutively from adipocytes and adipose tissue in both humans and mice. (v) Coulter Multisizer analyses revealed that the AGT mRNA level in MAs was correlated inversely with the average size of adipocytes larger than the nadir of bimodal histograms.

As AGT is secreted from many organs including liver, kidney, and vascular cells,[1,2] contribution of adipose tissue to plasma AGT level has not been determined. Furthermore, precise measurements of plasma AGT level were not conducted; instead, the radioimmunoassay result for angiotensin I has long been used as an equivalent.[1,17] In this context, an accurate assessment of A-AGT-S is critical for investigating clinical implications of adipose tissue RAS. Using a newly developed ELISA,[9,10] this study demonstrated for the first time that AGT was secreted constitutively from adipocytes and adipose tissue (**Supplementary Figures S3** online). Based on our novel finding, A-AGT-S was estimated by multiplying the mRNA level of AGT/g adipose tissue and fat mass or serum leptin, where applicable. Notably, only AGT is nutritionally regulated in adipose tissue from mice among RAS components (**Figure 2a,b,e–h**) reinforcing the rationale for focusing on A-AGT-S.

In this study, plasma AGT levels were increased ~20% in the obese mouse, whereas they were decreased ~12% in mice with weight reduction. A-AGT-S in EF, SF, MF, and RF was correlated with plasma AGT (**Figure 3e–h**). In contrast, AGT mRNA levels in the liver, kidney, and aorta were not altered in body weight changes (**Figure 2c,d**), suggesting adipose tissue–specific regulation of AGT in obesity. Under caloric intervention, changes in weights in the liver and kidney were subtle compared to fat depots, supporting the notion that AGT from the liver and kidney may not vary considerably in obesity or weight reduction. Taken together, it is reasonable to speculate that A-AGT-S contributes considerably (~20%) to plasma AGT level, accompanied by an increase in body fat mass.

Nevertheless the notion that visceral fat contributes to only ~10% of total adipose tissue mass in nonobese humans,[18] visceral adipose tissue–derived AGT secretion would not be negligible. In this context, in mouse models, we analyzed A-AGT-S in EF, MF, and RF, in addition to SF. A-AGT-S in EF, MF, and RF was increased in obese mice, whereas decreased in mice with weight reduction, and the A-AGT-S value in each adipose depot was correlated with plasma AGT level. Based on these results, it is likely to speculate that visceral adipose tissue–derived AGT secretion, like subcutaneous adipose tissue–derived AGT secretion, is substantially augmented and contributes to the plasma AGT level in human obesity.

Adipose tissue AGT mRNA levels were decreased by obesity and increased by weight loss, whereas A-AGT-S showed the opposite trend (**Figures 1–3**). It is likely that increased mass of adipose tissue in obesity overwhelmed the decrease in AGT expression, resulting in an increase in A-AGT-S and plasma AGT. Increased leptin mRNA level contributes to the extreme elevation of plasma leptin level in obesity.[19] Distinct from leptin, it is reasonable to speculate that AGT mRNA in adipose tissue is regulated so that plasma AGT concentration does not rise extremely in obesity. Although a series of hormonal and inflammatory changes may control AGT expression in adipose tissue,[1,20] the mechanism whereby AGT mRNA level is decreased exclusively in obese adipose tissue still remains obscure.

The mechanistic link between adipocyte size and metabolic consequences has long stimulated great interest in research.[11,12] To date, most of studies have employed histological analyses for assessing adipocyte size.[8,11] However, it should be noted that the distribution of adipocyte diameter is bimodal in humans.[12,13] Therefore, in this study, adipocyte size was analyzed using a Coulter Multisizer, which allows determination of the distribution of adipocyte size with greatest accuracy.[12] The progression of obesity is tightly associated with adipocyte hypertrophy.[21] In agreement with this notion, the average size of adipocytes larger than the nadir[12] was correlated with BMI ($r = 0.51$, $P = 0.03$), indicating that an increase in the average size of larger adipocytes tightly reflects adipocyte hypertrophy. The AGT mRNA level in isolated MAs was inversely correlated with the average size of larger adipocytes in humans (**Figure 4d**). We recently found that the AGT mRNA level was decreased in a long-term culture (~28 days) of 3T3–L1 adipocytes, with a concomitant increase in cellular triglyceride content (S. Okada, C. Kozuka, H. Masuzaki, S. Yasue, T. Ishii-Yonemato, Y. Yamamoto, M. Noguchi, T. Kusakabe, T. Tomita, J. Fujikura, K. Ebihara, K. Hosoda, H. Sakaue, H. Kobori, M. Ham, Y. Sok Lee, J. Bum Kim, Y. Saito, and K. Nakao, unpublished data). Although further studies are warranted, triglyceride accumulation and adipocyte hypertrophy may contribute to a decrease in AGT mRNA expression in obese adipose tissue.

In summary, this study is the first to demonstrate that secretion of adipose tissue–derived AGT is substantially augmented and contributes to the plasma AGT level in both obese humans and obese mice. Our results suggest that increase in adipose tissue–derived AGT contributes to circulating AGT level and resultant pathophysiology of obesity-related metabolic diseases.

Supplementary material is linked to the online version of the paper at http://www.nature.com/ajh

Acknowledgments: We are grateful to Mrs A. Ryu, S. Maki, and Ms. M. Nagamoto for assistance. This work was supported in part by a Grant-in-Aid for Scientific Research (B2), Takeda Medical Research Foundation, and Lilly Research Foundation. Clinical Trial Registration Number: UMIN000001969.

Disclosure: The authors declared no conflict of interest.

1. Engeli S, Schling P, Gorzelniak K, Boschmann M, Janke J, Ailhaud G, Teboul M, Massiéra F, Sharma AM. The adipose-tissue renin-angiotensin-aldosterone system: role in the metabolic syndrome? *Int J Biochem Cell Biol* 2002; 35: 807–825.
2. Dzau VJ. Circulating versus local renin-angiotensin system in cardiovascular homeostasis. *Circulation* 1988; 77:4–13.
3. Kurtz TW. Beyond the classic angiotensin-receptor-blocker profile. *Nat Clin Pract Cardiovasc Med* 2008; 5 Suppl 1:S19–S26.
4. Yusuf S, Sleight P, Pogue J, Bosch J, Davies R, Dagenais G. Effects of an angiotensin-converting-enzyme inhibitor, ramipril, on cardiovascular events in high-risk patients. The Heart Outcomes Prevention Evaluation Study Investigators. *N Engl J Med* 2000; 20:145–153.
5. Ogihara T, Nakao K, Fukui T, Fukiyama K, Saruta T. Clinical outcomes in hypertensive patients with high cardiovascular risks: principal results of candesartan antihypertensive survival evaluation in Japan (CASE-J) study. In: The 21st Scientific Meeting of the International Society of Hypertension, Fukuoka, Japan, 2006.
6. Massiera F, Bloch-Faure M, Ceiler D, Murakami K, Fukamizu A, Gasc JM, Quignard-Boulange A, Negrel R, Ailhaud G, Seydoux J, Meneton P, Teboul M. Adipose angiotensinogen is involved in adipose tissue growth and blood pressure regulation. *FASEB J* 2001; 15:2727–2729.
7. Giacchetti G, Faloia E, Mariniello B, Sardu C, Gatti C, Camilloni MA, Guerrieri M, Mantero F. Overexpression of the renin-angiotensin system in human visceral adipose tissue in normal and overweight subjects. *Am J Hypertens* 2002; 15:381–388.
8. Hainault I, Nebout G, Turban S, Ardouin B, Ferre P, Quignard-Boulange A. Adipose tissue-specific increase in angiotensinogen expression and secretion in the obese (fa/fa) Zucker rat. *Am J Physiol Endocrinol Metab* 2002; 282:E59–E66.
9. Katsurada A, Hagiwara Y, Miyashita K, Satou R, Miyata K, Ohashi N, Navar LG, Kobori H. Novel sandwich ELISA for human angiotensinogen. *Am J Physiol Renal Physiol* 2007; 293:F956–F960.
10. Kobori H, Katsurada A, Miyata K, Ohashi N, Satou R, Saito T, Hagiwara Y, Miyashita K, Navar LG. Determination of plasma and urinary angiotensinogen levels in rodents by newly developed ELISA. *Am J Physiol Renal Physio* 2008; 294: F1257–F1263.
11. Jernås M, Palming J, Sjöholm K, Jennische E, Svensson PA, Gabrielsson BG, Levin M, Sjögren A, Rudemo M, Lystig TC, Carlsson B, Carlsson LM, Lönn M. Separation of human adipocytes by size: hypertrophic fat cells display distinct gene expression. *FASEB J* 2006; 20:1540–1542.
12. McLaughlin T, Sherman A, Tsao P, Gonzalez O, Yee G, Lamendola C, Reaven GM, Cushman SW. Enhanced proportion of small adipose cells in insulin-resistant vs insulin-sensitive obese individuals implicates impaired adipogenesis. *Diabetologia* 2007; 50:1707–1715.
13. Julien P, Despres JP, Angel A. Scanning electron microscopy of very small fat cells and mature fat cells in human obesity. *J Lipid Res* 1989; 30:293–299.
14. Arai N, Masuzaki H, Tanaka T, Ishii T, Yasue S, Kobayashi N, Tomita T, Noguchi M, Kusakabe T, Fujikura J, Ebihara K, Hirata M, Hosoda K, Hayashi T, Sawai H, Minokoshi Y, Nakao K. Ceramide and adenosine 5′-monophosphate-activated protein kinase are two novel regulators of 11β-hydroxysteroid dehydrogenase type 1 expression and activity in cultured preadipocytes. *Endocrinology* 2007; 148:5268–5277.
15. Friedman JM, Halaas JL. Leptin and the regulation of body weight in mammals. *Nature* 1998; 395:763–770.
16. Masuzaki H, Ogawa Y, Isse N, Satoh N, Okazaki T, Shigemoto M, Mori K, Tamura N, Hosoda K, Yoshimasa Y, Jingami H, Kawada T, Nakao K. Human obese gene expression. Adipocyte-specific expression and regional differences in the adipose tissue. *Diabetes* 1995; 44:855–858.
17. Umemura S, Nyui N, Tamura K, Hibi K, Yamaguchi S, Nakamaru M, Ishigami T, Yabana M, Kihara M, Inoue S, Ishii M. Plasma angiotensinogen concentrations in obese patients. *Am J Hypertens* 1997; 10:629–633.
18. Wajchenberg BL. Subcutaneous and visceral adipose tissue: their relation to the metabolic syndrome. *Endocr Rev* 2000; 21:697–738.
19. Lönnqvist F, Nordfors L, Jansson M, Thörne A, Schalling M, Arner P. Leptin secretion from adipose tissue in women. Relationship to plasma levels and gene expression. *J Clin Invest* 1997; 99:2398–2404.
20. Aubert J, Darimont C, Safonova I, Ailhaud G, Negrel R. Regulation by glucocorticoids of angiotensinogen gene expression and secretion in adipose cells. *Biochem J* 1997; 328:701–706.
21. Bays HE, González-Campoy JM, Bray GA, Kitabchi AE, Bergman DA, Schorr AB, Rodbard HW, Henry RR. Pathogenic potential of adipose tissue and metabolic consequences of adipocyte hypertrophy and increased visceral adiposity. *Expert Rev Cardiovasc Ther* 2008; 6:343–368.

Available online at www.sciencedirect.com
ScienceDirect
Metabolism Clinical and Experimental 59 (2010) 1241–1251
Metabolism
Clinical and Experimental
www.metabolismjournal.com

# Adipose tissue–specific dysregulation of angiotensinogen by oxidative stress in obesity

Sadanori Okada[a,b,1], Chisayo Kozuka[a,1], Hiroaki Masuzaki[a,*], Shintaro Yasue[a], Takako Ishii-Yonemoto[a], Tomohiro Tanaka[a], Yuji Yamamoto[a], Michio Noguchi[a], Toru Kusakabe[a], Tsutomu Tomita[a], Junji Fujikura[a], Ken Ebihara[a], Kiminori Hosoda[a], Hiroshi Sakaue[c], Hiroyuki Kobori[d], Mira Ham[e], Yun Sok Lee[e], Jae Bum Kim[e], Yoshihiko Saito[b], Kazuwa Nakao[a]

[a]*Department of Medicine and Clinical Science, Kyoto University Graduate School of Medicine, Kyoto 606-8507, Japan*
[b]*First Department of Internal Medicine, Nara Medical University, Kashihara 634-8522, Japan*
[c]*Department of Nutrition and Metabolism, Institute of Health Biosciences, The University of Tokushima Graduate School, Tokushima 770-8503, Japan*
[d]*Departments of Medicine and Physiology, and Hypertension and Renal Center of Excellence, Tulane University Health Sciences Center, New Orleans, LA 70112-2699, USA*
[e]*Institute of Molecular Biology and Genetics, Seoul National University, Seoul 110-744, South Korea*

Received 27 August 2009; accepted 18 November 2009

**Abstract**

Adipose tissue expresses all components of the renin-angiotensin system including angiotensinogen (AGT). Recent studies have highlighted a potential role of AGT in adipose tissue function and homeostasis. However, some controversies surround the regulatory mechanisms of AGT in obese adipose tissue. In this context, we here demonstrated that the AGT messenger RNA (mRNA) level in human subcutaneous adipose tissue was significantly reduced in obese subjects as compared with nonobese subjects. Adipose tissue AGT mRNA level in obese mice was also lower as compared with their lean littermates; however, the hepatic AGT mRNA level remained unchanged. When 3T3-L1 adipocytes were cultured for a long period, the adipocytes became hypertrophic with a marked increase in the production of reactive oxygen species. Expression and secretion of AGT continued to decrease during the course of adipocyte hypertrophy. Treatment of the 3T3-L1 and primary adipocytes with reactive oxygen species (hydrogen peroxide) or tumor necrosis factor α caused a significant decrease in the expression and secretion of AGT. On the other hand, treatment with the antioxidant *N*-acetyl cysteine suppressed the decrease in the expression and secretion of AGT in the hypertrophied 3T3-L1 adipocytes. Finally, treatment of obese *db/db* mice with *N*-acetyl cysteine augmented the expression of AGT in the adipose tissue, but not in the liver. The present study demonstrates for the first time that oxidative stress dysregulates AGT in obese adipose tissue, providing a novel insight into the adipose tissue–specific interaction between the regulation of AGT and oxidative stress in the pathophysiology of obesity.


## 1. Introduction

Overactivity of the systemic renin-angiotensin system (RAS) is one of the central mechanisms for obesity-related metabolic disorders [1,2]. Notably, the major components of the RAS are expressed in various tissues including the heart, blood vessels, adipose tissue, and brain [3]; these comprise tissue RAS. A series of products are produced locally from

The authors of this manuscript have nothing to declare.

Institutional approval: The human study was approved by the ethics committee for human research of the Kyoto University Graduate School of Medicine (2004, no. 553). Written informed consent was obtained from all subjects prior to the study. All animal experimental procedures were approved by the Kyoto University Graduate School of Medicine Animal Research Committee and the Seoul National University Animal Experiment Ethics Committee.

* Corresponding author. Division of Endocrinology and Metabolism, Second Department of Internal Medicine, Faculty of Medicine, University of the Ryukyus, Okinawa 903-0215, Japan. Tel.: +81 98 895 1145; fax: +81 98 895 1415.
*E-mail address:* hiroaki@med.u-ryukyu.ac.jp (H. Masuzaki).

[1] Sadanori Okada and Chisayo Kozuka contributed equally to this work.

0026-0495/$ – see front matter © 2010 Elsevier Inc. All rights reserved.
doi:10.1016/j.metabol.2009.11.016

angiotensinogen (AGT), the unique precursor of angiotensin peptides, and play a critical role in cardiovascular homeostasis [3,4].

Although AGT is produced mainly by the liver, adipose tissue is also considered as a source of AGT production [5]. In agreement with this notion, the adipose tissue expresses all components of the RAS, including AGT, renin, angiotensin I–converting enzyme, and angiotensin II type 1 receptor, in humans and rodents [6,7]. A previous study has demonstrated that AGT-deficient mice are low in blood pressure and body fat mass [8]. Moreover, adipocyte-specific transgenic overexpression of AGT on an AGT-deficient background was shown to augment plasma AGT level and rescue hypotension and leanness [9]. These results indicate that adipose tissue–derived AGT does contribute to the circulating AGT level and adipogenesis.

In rodent experiments, the AGT messenger RNA (mRNA) level in white adipose tissue has been shown to be regulated by the nutritional status; however, that in the liver was independent of the nutritional status [10,11]. In human cross-sectional studies, the AGT mRNA level in adipose tissue was shown to be higher in obese subjects [6,12]. On the other hand, another study reported that the AGT mRNA level in adipose tissue was significantly lower in obese individuals [13]. Elevation of AGT expression in adipose tissue in obese individuals thus remains controversial [14].

Several studies have shown that increased oxidative stress is a manifestation of obesity-related metabolic derangement [15-17]. In fact, in humans, oxidative stress is critically associated with atherosclerosis, hypertension, and diabetes mellitus [18,19]. Oxidative stress is also related with the RAS. Angiotensin II is a potent inducer of reactive oxygen species (ROS) in a variety of tissues [20-22]. In the liver and kidney, increased ROS has been reported to increase AGT gene expression [23-26]. Also in obese adipose tissue, generation of ROS is exaggerated and is involved in adipose tissue dysfunction [17,27]. However, whether increased ROS may affect adipose AGT production remains to be elucidated.

In the present study, we demonstrated that the AGT mRNA level was reduced in obese adipose tissue in humans and mice and in hypertrophied 3T3-L1 adipocytes. In this context, we tested the hypothesis that increased oxidative stress would modulate AGT in obese adipose tissue.

## 2. Materials and methods

### *2.1. Subcutaneous abdominal adipose tissue biopsies in human subjects*

The present study was performed according to the Declaration of Helsinki and approved by the Ethical Committee on Human Research of Kyoto University Graduate School of Medicine (2004, no. 553). Written informed consent was obtained from all subjects before the study.

Subcutaneous abdominal adipose tissue biopsies were obtained from 46 Japanese subjects (24 men and 22 women; age [mean ± SD], 46 ± 2.1 years). The body mass index (BMI) of the subjects ranged from 19 to 52 (mean ± SD, 30 ± 1.6) kg/m$^2$. All subjects had been on stable therapy with lipid-lowering, antihypertensive, or hypoglycemic agents for at least 1 month before admission and continued with the same doses throughout the study period. Patients who received angiotensin I–converting enzyme inhibitors, angiotensin II receptor blockers, and steroid-related drugs were carefully excluded. For the study, subcutaneous abdominal adipose depots of the study subjects were excised from the periumbilical region under local anesthesia. The samples were immediately frozen in liquid nitrogen and stored at −80°C until use.

### *2.2. Mouse experiments*

Male *ob/ob* mice (age, 12 weeks) were purchased from Oriental BioService (Kyoto, Japan) and housed in the animal facility of Kyoto University. Male *db/db* mice (age, 10 weeks) were purchased from Japan SLC (Hamamatsu, Japan) and housed in Seoul National University. The mice were allowed free access to food and water. For in vivo antioxidant treatment, the *db/db* mice were injected with *N*-acetyl cysteine (NAC; 150 mg/kg body weight; Sigma-Aldrich Japan, Tokyo, Japan) or the vehicle (phosphate-buffered saline) into the peritoneal cavity once daily for 1 week. All experimental procedures were approved by the Kyoto University Graduate School of Medicine Animal Research Committee and the Seoul National University Animal Experiment Ethics Committee.

### *2.3. Cell culture and isolation of primary adipocytes*

3T3-L1 fibroblasts were cultured and differentiated into adipocytes as described previously [28]. Briefly, the 2-day postconfluent cells (designated as day 0) were incubated for 2 days with 10% fetal bovine serum (FBS)/Dulbecco modified Eagle medium (DMEM), 0.5 mmol/L 3-isobutyl-1-methylxanthine, 0.25 μmol/L dexamethasone, and 1 μg/mL insulin. The cells were then incubated for 2 days in 10% FBS/DMEM with insulin and, thereafter, incubated in 10% FBS/DMEM that was changed on every alternate day. Oil red O staining was performed as described [29].

Primary adipocytes were isolated from epididymal fat pads of 9-week-old male C57BL/6J mice (purchased from Oriental BioService, Kyoto, Japan). Epididymal fat pads were harvested, minced into 2- to 3-mm pieces, and digested using 0.8 mg/mL collagenase (Sigma-Aldrich Japan) in DMEM for 30 minutes at 37°C in a shaking water bath. After the digestion with collagenase, cells were filtered through a 250-μm nylon filter and centrifuged at 1000 rpm for 30 seconds. The suspended mature adipocytes were separated from the pelleted stromovascular fraction and washed 3 times in DMEM for experiments.

### 2.4. Determination of adipocyte size

The cells were fixed with 2% osmium tetroxide and passed through a 250-μm nylon filter to remove the fibrous elements, and the cells were washed extensively with isotonic saline. A total of 10 000 cells was analyzed using the Coulter Multisizer III (Beckman Coulter, High Wycombe, England) [30].

### 2.5. Quantitative real-time polymerase chain reaction

Total RNA was extracted from human and mouse adipose tissue by using a QIAGEN RNeasy Mini Kit (QIAGEN Japan, Tokyo, Japan) and from cultured adipocytes by using Trizol Reagent (Invitrogen, Carlsbad, CA). Complementary DNA was then synthesized by using an iScript cDNA Synthesis Kit (Bio-Rad, Hercules, CA). Taqman polymerase chain reactions (PCRs) for human AGT, mouse AGT, mouse monocyte chemoattractant protein 1 (MCP-1), mouse interleukin 6 (IL-6), and mouse tumor necrosis factor α (TNFα) were performed using the ABI Prism 7300 Sequence Detection System (Applied Biosystems, Foster City, CA). The sequences of probes and primers are summarized in Table 1.

### 2.6. Enzyme-linked immunosorbent assay

The AGT protein level in the culture media was measured by sandwich-type enzyme-linked immunosorbent assay (ELISA) as described [31]. Similarly, the MCP-1 and IL-6 protein levels were detected by using an ELISA kit (R&D Systems, Minneapolis, MN).

### 2.7. Determination of ROS

The ROS activity was determined by the nitroblue tetrazolium (NBT) assay [32]. Reduced NBT (formazan) was dissolved in 50% acetic acid, and the absorbance of the supernatant was determined at 560 nm.

### 2.8. Statistical analysis

The data are presented as the mean ± SE. Unpaired Student $t$ test was used for comparisons with the control group. The differences were accepted as significant at a level of $P < .05$.

## 3. Results

### 3.1. AGT mRNA expression level in adipose tissue from obese humans and mice

To explore the impact of obesity on AGT gene expression in human adipose tissue, we performed subcutaneous abdominal adipose tissue biopsies from 46 subjects with a wide range of BMI. The AGT mRNA level was significantly reduced by 61% in the obese subjects as compared with the nonobese subjects (Fig. 1A).

To verify the obesity-related decrease in adipose AGT expression, we analyzed adipose tissue from genetically obese mice. In 12-week-old male *ob/ob* mice (mean body weight, 60 ± 0.7 g), the AGT mRNA level was significantly decreased in both epididymal (29%) and subcutaneous (57%) adipose depots as compared with their lean littermates (mean body weight, 29 ± 0.3 g) (Fig. 1B). On the other hand, the AGT mRNA levels in the liver remained unaltered in both groups (Fig. 1C).

Similar results were observed in case of the diet-induced obese (DIO) mice (12-week-old male C57BL/6J mice fed with a high-fat/high-sucrose diet for 4 weeks). The AGT mRNA level in the adipose tissue of the DIO mice (mean body weight, 40 ± 0.8 g) was significantly lower than that in the adipose tissue of their lean littermates (mean body weight, 30 ± 0.4 g) ($P < .05$); however, the hepatic AGT mRNA level remained unchanged in both groups (Yasue et al, unpublished observations). These results indicate that the AGT mRNA level was decreased exclusively in the obese adipose tissue in both humans and mice.

### 3.2. AGT expression during the course of hypertrophy in the 3T3-L1 adipocytes

To explore the mechanism by which AGT is decreased in obese adipose tissue, we analyzed hypertrophied adipocytes. 3T3-L1 fibroblasts were completely differentiated into

Table 1
Sequences of Taqman PCR primers and probes

| Gene name<br>Genbank accession no. | Forward primer<br>Reverse primer | Probe (5′-FAM, 3′-TAMRA) |
|---|---|---|
| Human AGT<br>NM_000029 | GGTGGAGGGTCTCACTTTCCA<br>ATGGTCAGGTGGATGGTCCG | CCCTCAACTGGATGAAGAAACTGTCTCC |
| Mouse Agt<br>NM_007428 | ACACCTACGTTCACTTCCAAG<br>CCGAGATGCTGTTGTCCAC | ATGAGAGGTTTCTCTCAGCTGCCTGGA |
| Mouse Ccl2 (MCP-1)<br>NM_011333 | TTGGCTCAGCCAGATGC<br>CCAGCCTACTCATTGGGATCA | CCCCACTCACCTGCTGCTACTCATTCA |
| Mouse Il6 (IL-6)<br>NM_031168 | ATGAAGTTCCTCTCTGCAAGAG<br>GTAGGGAAGGCCGTGGTTG | CACCAGCATCAGTCCCAAGAAGGCA |
| Mouse Tnf (TNFα)<br>NM_013693 | TCTCTTCAAGGGACAAGGCTG<br>ATAGCAAATCGGCTGACGGT | CCCGACTACGTGCTCCTCACCCA |

The sequences of primers and probes for each gene used in the present study are summarized.

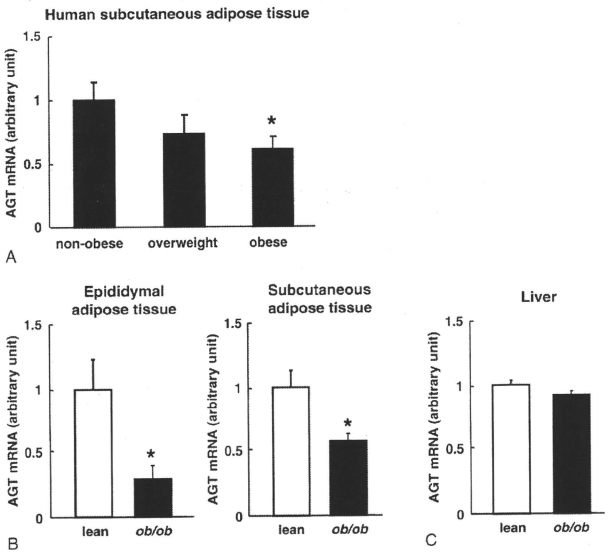


Fig. 1. The AGT mRNA levels in obese adipose tissue from humans and mice. A, The relation between the AGT mRNA level in subcutaneous abdominal adipose tissue and the degree of obesity in humans: nonobese (BMI <25), n = 20; overweight (25 ≤ BMI < 30), n = 13; obese (BMI ≥30), n = 13. B, Comparison of the adipose tissue AGT mRNA levels in 12-week-old male *ob/ob* mice (n = 4; mean body weight, 60 ± 0.7 g) and their lean littermates (n = 4; mean body weight, 29 ± 0.3 g). Left: epididymal adipose tissue depots. Right: subcutaneous abdominal adipose tissue depots. C, Comparison of the hepatic AGT mRNA level between the *ob/ob* mice (n = 4) and their lean littermates (n = 4). The mRNA level was examined by real-time PCR and normalized to that of 18S ribosomal RNA (rRNA). The data are expressed as the mean ± SE. $^*P < .05$ as compared with the nonobese subjects or the lean littermates.

adipocytes for 8-day incubation with induction media [28]. Consistent with a previous report [33], the AGT mRNA level in differentiated 3T3-L1 adipocytes (day 8) was significantly elevated by 15-folds in comparison with 3T3-L1 fibroblasts (day 0). For generating hypertrophied adipocytes, 3T3-L1 adipocytes were cultured up to 30 days after the induction of differentiation. Oil red O staining exhibited a gradual increase in lipid accumulation from day 8 to day 28. The adipocytes displayed unilocular lipid droplets on days 18 and 28 (Fig. 2A).

The mean diameter of the adipocytes as assessed by the Coulter Multisizer III was 20.2 μm on day 8 and 37.5 μm on day 30 (Fig. 2B). During the course of adipocyte hypertrophy, ROS production increased 2.7-folds (day 18) and 4.3-folds (day 28) in comparison with the levels on day 8 (Fig. 2C). The mRNA and protein levels of MCP-1 and IL-6 were elevated substantially on days 18 and 28 (Fig. 2D and E, respectively). The AGT mRNA level was significantly lower on days 18 (48%) and 28 (42%) than that on day 8 (Fig. 2D). The AGT concentration in the culture media was decreased on days 18 (59% of the initial value) and 28 (42% of the initial value) (Fig. 2E). These results suggest that AGT expression and secretion were decreased in the hypertrophied adipocytes.

### *3.3. Impact of TNFα on the expression and secretion of AGT in adipocytes*

Tumor necrosis factor α plays a critical role in the pathophysiology of inflammation and oxidative stress [27,34,35]. To explore the impact of TNFα on the expression and secretion of AGT in adipocytes, the differentiated 3T3-L1 adipocytes (day 8) were treated with TNFα (Sigma-Aldrich Japan) for 24 hours. Treatment with TNFα decreased the AGT mRNA level in a dose-dependent manner along with a concomitant increase in the MCP-1 and IL-6 mRNA levels (Fig. 3A). The AGT protein level in the culture media decreased in parallel to the AGT mRNA level (Fig. 3B).

We also investigated the effects of TNFα on primary adipocytes. Similarly to 3T3-L1 adipocytes, treatment with TNFα (10 ng/mL) for 24 hours slightly but significantly decreased AGT mRNA level and substantially increased MCP-1 mRNA level (Fig. 3C).

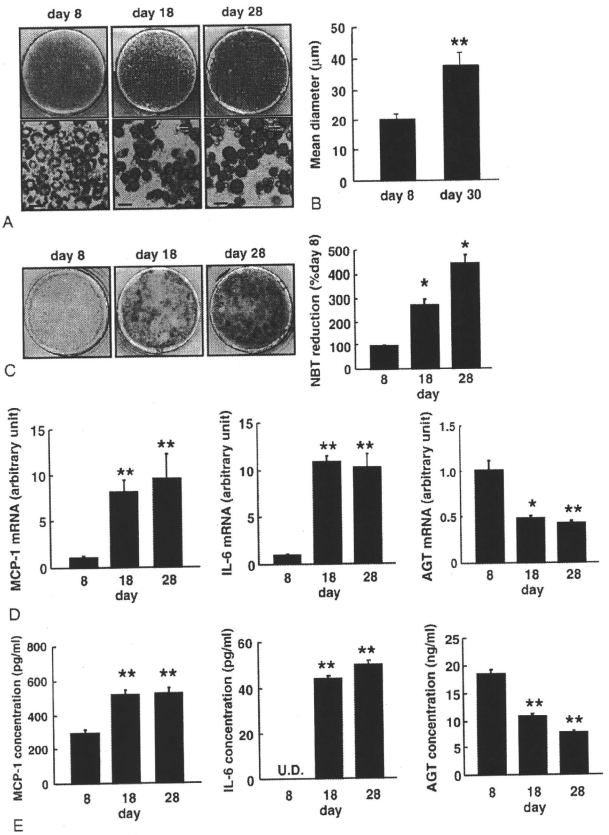


Fig. 2. The AGT expression during the course of hypertrophy in the 3T3-L1 adipocytes. A, Oil red O staining of the 3T3-L1 adipocytes on days 8, 18, and 28 after induction of differentiation. Bar = 30 μm. B, Size of the 3T3-L1 adipocytes on days 8 and 30. Adipocyte size was measured using a Coulter Multisizer III. C, The ROS production during adipocyte hypertrophy. The ROS production was assessed by the NBT assay. Dark blue formazan was dissolved, and the absorbance was determined at 560 nm (n = 3). D, The MCP-1, IL-6, and AGT mRNA levels in the 3T3-L1 adipocytes on days 8, 18, and 28 (n = 4). The mRNA level was examined by real-time PCR and normalized to that of 18S rRNA. E, The AGT protein concentration in the culture media. The MCP-1, IL-6, and AGT concentrations in the 3T3-L1 adipocytes on days 8, 18, and 28 were analyzed by ELISA (n = 4). Results are representatives of at least 3 independent experiments. The data are expressed as the mean ± SE. $*P < .05$ and $**P < .01$ as compared with the value of day 8. U.D. indicates undetectable.

### *3.4. Impact of oxidative stress on the expression and secretion of AGT in adipocytes*

To explore the impact of oxidative stress on the expression and secretion of AGT in adipocytes, differentiated 3T3-L1 adipocytes (day 8) were exposed to a specific ROS molecule, hydrogen peroxide ($H_2O_2$), for 24 hours [17,36]. Incubation of adipocytes with $H_2O_2$ significantly increased the MCP-1 mRNA level, consistent with a previous report [17]. In contrast, $H_2O_2$ diminished the AGT mRNA level up to 35% of the initial value in a dose-dependent manner (Fig. 4A). The AGT protein level in the

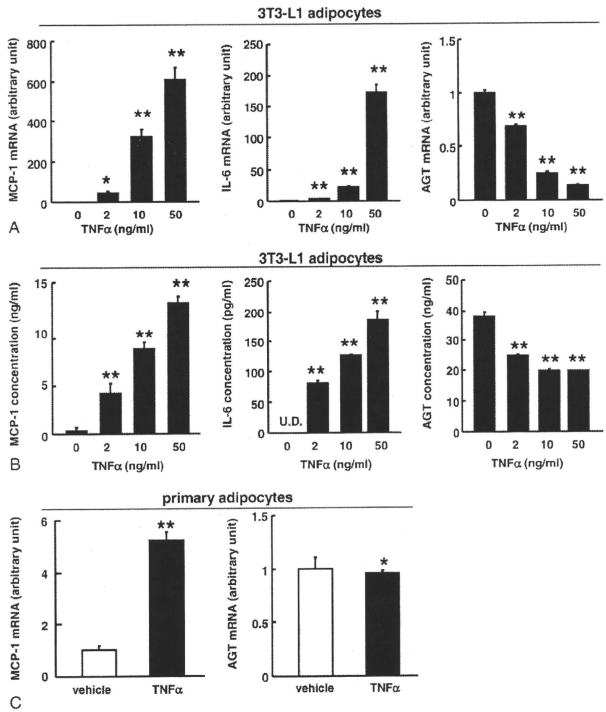


Fig. 3. Impact of TNFα on the expression and secretion of AGT in the 3T3-L1 adipocytes. A, The AGT, MCP-1, and IL-6 mRNA level in the 3T3-L1 adipocytes (day 8) treated with TNFα for 24 hours (n = 4). The mRNA level was examined by real-time PCR and normalized to that of 18S rRNA. B, The AGT protein concentration in the culture media in the 3T3-L1 adipocytes (day 8) treated with TNFα for 24 hours (n = 4). The protein level was assessed by ELISA. C, The AGT and MCP-1 mRNA level in the primary adipocytes treated with TNFα (10 ng/mL) for 24 hours (n = 4). The mRNA level was examined by real-time PCR and normalized to that of 18S rRNA. Results are representatives of at least 3 independent experiments. The data are expressed as the mean ± SE. $*P < .05$ and $**P < .01$ as compared with the control value.

culture media also decreased up to 23% of the initial value (Fig. 4B).

Similar to 3T3-L1 adipocytes, $H_2O_2$ treatment (1 mmol/L, 24 hours) significantly decreased AGT mRNA level in primary adipocytes (Fig. 4C). The $H_2O_2$ treatment tended to increase the MCP-1 mRNA level.

### 3.5. Effect of antioxidant treatment on the expression and secretion of AGT in adipocytes

We examined whether inhibition of ROS generation could nullify the decrease in AGT gene expression and AGT secretion in obese adipose tissue. First, we treated 3T3-L1 adipocytes with the antioxidant NAC (10 mmol/L) for 10 days (days 8-18). Without the NAC treatment, the adipocytes had become hypertrophic and increased ROS production in this period (Fig. 2B and C). The NBT assay revealed that NAC treatment significantly suppressed ROS production (Fig. 5A). Although ROS production was reported to potentiate adipocyte differentiation in early phase [37], the ROS suppression with the NAC treatment in our experiments did not cause morphologic changes in hypertrophied adipocytes compared with the vehicle treatment. The NAC treatment inhibited the increase in MCP-1 expression (Fig. 5B). The AGT mRNA level was significantly elevated with NAC treatment (Fig. 5B).

To test whether such phenomenon is reproducible in obese adipose tissue where ROS production is exaggerated

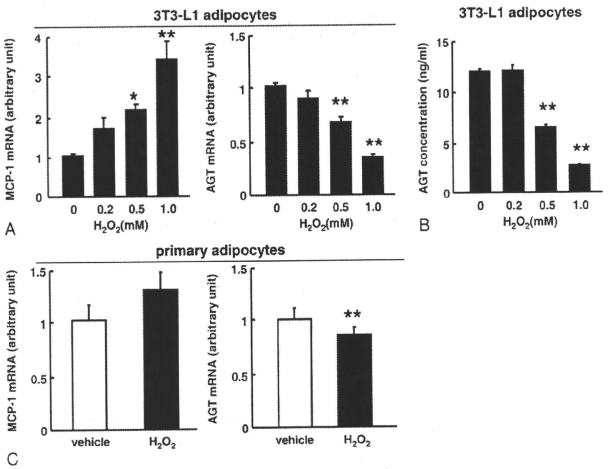


Fig. 4. Impact of oxidative stress on the expression and secretion of AGT in the 3T3-L1 adipocytes. A, The AGT and MCP-1 mRNA level in the 3T3-L1 adipocytes (day 8) treated with $H_2O_2$ for 24 hours (n = 4). The mRNA level was examined by real-time PCR and normalized to that of 18S rRNA. B, The AGT protein level in the culture media of the 3T3-L1 adipocytes (day 8) treated with $H_2O_2$ for 24 hours (n = 4). The protein concentration was assessed by ELISA. C, The AGT and MCP-1 mRNA level in the primary adipocytes treated with $H_2O_2$ (1 mmol/L) for 24 hours (n = 4). The mRNA level was examined by real-time PCR and normalized to that of 18S rRNA. Results are representatives of at least 3 independent experiments. The data are expressed as the mean ± SE. $^*P < .05$ and $^{**}P < .01$ as compared with the control value.

[17], we administered NAC to obese *db/db* mice once daily for 1 week. Similar to the obese *ob/ob* mice and DIO mice, in obese *db/db* mice (mean body weight, 48 ± 1.5 g), the AGT mRNA level in epididymal adipose tissue was markedly decreased to 22% as compared with their lean littermates (mean body weight, 28 ± 1.0 g) (Fig. 5C). In contrast, the TNFα mRNA level in epididymal adipose tissue was significantly higher in *db/db* mice than in their lean littermates (Fig. 5C). Both systemic and local (adipose tissue) oxidative stress was elevated substantially in obese *db/db* mice [38]. Notably, in *db/db* mice, NAC treatment significantly reduced the oxidative stress also in adipose tissue [38].

In the NAC treatment group, the AGT mRNA level in the epididymal adipose depots increased significantly by 2.1-folds compared with that in the vehicle group, whereas the IL-6 ($P = .052$) and TNFα ($P = .10$) mRNA levels tended to decrease in the NAC treatment group (Fig. 5D). On the other hand, the hepatic AGT mRNA level remained unchanged in both groups (Fig. 5E).

## 4. Discussion

The major finding of the present study is that oxidative stress dysregulates AGT in adipose tissue in obese humans and rodents. The AGT mRNA level was decreased in both obese adipose tissue and hypertrophied adipocytes, in which oxidative stress was exaggerated. Exposure of oxidative stress decreased AGT expression not only in the adipocyte cell line but also in primary adipocytes. The decrease in AGT expression was rescued by treatment with the antioxidant both in vivo and in vitro. Such obesity-associated changes in AGT in the adipose tissue were not observed in the liver.

The AGT regulation in obese adipose tissue has long been analyzed, but results were inconsistent [6,12,13]. We here demonstrated that the AGT mRNA level in adipose tissue was reduced in both obese humans and mice (Fig. 1). In obese mice, there seem to be no apparent depot-specific (subcutaneous and epididymal adipose depots) or strain-specific (*ob/ob*, *db/db*, and DIO mice) differences in the fall of AGT in adipose tissue. The AGT mRNA level was decreased also in hypertrophied 3T3-L1 adipocytes (Fig. 2). These results are consistent with a previous report using differentiation system of human adipocytes in primary culture, where the AGT mRNA level increased in differentiation process, but decreased in further culture process [39].

In previous experiments, several hormonal and metabolic changes associated with obesity influence AGT expression in adipocytes; however, due to species differences and experimental conditions, there are controversies around the results [39-42]. On the other hand, our results indicate that

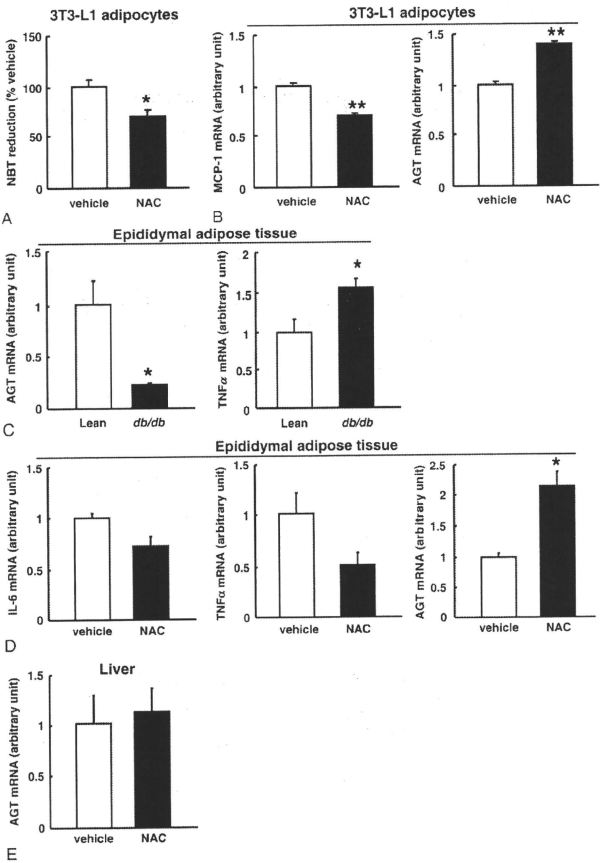


Fig. 5. Effect of antioxidant treatment on the expression and secretion of AGT in the adipocytes. A, Suppression of ROS generation in the 3T3-L1 adipocytes treated with NAC (10 mmol/L) for 10 days (n = 3). The ROS was estimated by the NBT assay. B, The MCP-1 and AGT mRNA levels in the 3T3-L1 adipocytes incubated with NAC (10 mmol/L) (n = 8). The mRNA level was examined by real-time PCR and normalized to that of 18S rRNA. Results are representatives of at least 3 independent experiments. C, Comparison of the AGT and TNFα mRNA levels between 10-week-old male *db/db* mice (n = 4; mean body weight, 48 ± 1.5 g) and their lean littermates (n = 4; mean body weight, 28 ± 1.0 g) in epididymal adipose tissue. D, The level of IL-6, TNFα, and AGT mRNA in the epididymal adipose tissue depots of obese *db/db* mice treated with NAC (150 mg/kg body weight) or vehicle (phosphate-buffered saline) once daily for 1 week (n = 3). E, The AGT mRNA level in the liver of obese *db/db* mice treated with NAC or vehicle for 1 week (n = 3). The mRNA level was examined by real-time PCR and normalized to that of cyclophilin mRNA. The data are expressed as the mean ± SE. $^{*}P < .05$ and $^{**}P < .01$ as compared with the control value.

AGT expression is decreased in obese adipose tissue. Reactive oxygen species ($H_2O_2$) decreased AGT expression in both 3T3-L1 adipocytes and primary adipocytes (Fig. 4). On the other hand, elimination of ROS with antioxidant increased AGT expression not only in hypertrophied 3T3-L1 adipocytes but also in adipose tissue from obese mice (Fig. 5). The oxidative stress–mediated decrease in adipose AGT is reproduced in our various experiments.

Several studies have suggested the augmentation of AGT by oxidative stress in the liver and kidney. In the liver, angiotensin II is known to enhance AGT expression via ROS generation [23], resulting in a positive feedback loop of AGT production [43]. In addition, oxidative stress mediated by hyperglycemia and hypertension has been shown to augment the expression of AGT in the rodent kidney [25,26]. In turn, elevated expression of AGT has been shown to activate renal RAS and considerably contribute to renal injury [26]. On the other hand, our data support a notion that oxidative stress "decreases" expression and secretion of AGT in obese adipose tissue, implying that regulation of AGT in adipose tissue may be distinct from other tissues in response to oxidative stress.

The clinical or pathophysiologic implications of decreased AGT in obese adipose tissue still remain unclear. Although further studies are warranted, the notion that adipose tissue RAS is involved in the control of adipogenesis and adipose tissue mass [44] tempts us to speculate that tissue-specific decrease of AGT in obese adipose tissue may serve as a defense against further exacerbation of adiposity. In obese adipose tissue, exaggerated oxidative stress affects the expression of a variety of genes [17]. Representatively, ROS induces the proinflammatory TNFα but suppresses the anti-inflammatory adiponectin in murine adipose tissue [17]. Glutathione peroxidase 3 (GPx3), an antioxidant enzyme secreted from the adipose tissue and kidney, is known to be decreased by oxidative stress exclusively in adipose tissue in obese *db/db* mice [38]. Notably, in vivo administration of an antioxidant was shown to rescue the decrease in GPx3 expression only in adipose tissue, but not in the kidney [38]. In this context, AGT shares close similarity with adiponectin and GPx3 in terms of the response to oxidative stress in adipose tissue.

Tissue-specific dysregulation of AGT has also been observed in inflammatory response [45,46]. Hepatic AGT is shown to increase by inflammatory stimuli via the acute-phase responsive element (APRE) on the promoter region of the AGT gene [43,47]. In rats treated with lipopolysaccharide, AGT mRNA level was shown to increase in the liver, aorta, and adrenal gland, but remained unchanged in the kidney [45]. Furthermore, in transgenic mice with cardioselective overexpression of TNFα, expression of AGT was decreased exclusively in the heart [46]. In the present study, we demonstrated that TNFα decreased the expression and secretion of AGT in 3T3-L1 adipocytes (Fig. 3). Considering that chronic, low-grade inflammation is a manifestation of obese adipose tissue [48,49], our results suggest that AGT is inversely regulated by inflammation in obese adipose tissue.

Previous works have raised a possibility that the inflammatory responses to AGT in adipose tissue and liver are controlled by distinct mechanisms [50]. In cultured adipocytes, inflammatory signals transcriptionally decrease AGT by the inhibition of APRE [50]; however, in cultured hepatocytes, nuclear factor–κB signaling augments AGT by the activation of APRE [47]. Importantly, the intracellular signaling involved in oxidative stress and inflammation interact and share, at least in part, common pathways in a tissue-specific manner [18,19]. In this context, tissue-specific dysregulation of AGT by oxidative stress is reminiscent of the case in inflammatory signals; and a possible link between the dysregulation of AGT and oxidative stress in obese adipose tissue may provide a fresh clue to dissect the pathophysiology of obesity. For example, we would suggest the one possibility that oxidative stress–induced suppression of adipose tissue RAS via the decrease in AGT may control adipose tissue function including adipocyte differentiation, lipolysis, and local blood flow [44].

In summary, the present study demonstrates for the first time that oxidative stress dysregulates AGT in obese adipose tissue in humans and rodents as well as in cultured adipocytes with hypertrophy. Our results support a concept that oxidative stress–dependent decrease in AGT may be a unique facet of dysfunction in obese adipose tissue.

## Acknowledgment

We are grateful to A Katsurada (Departments of Medicine and Physiology, and Hypertension and Renal Center of Excellence, Tulane University Health Sciences Center, New Orleans, LA), M Tabuchi (Department of Pharmacology, Kinki University School of Medicine, Osaka-sayama, Japan), M Okada (Department of Internal Medicine, Kobe University Graduate School of Medicine, Kobe, Japan), and M Kasuga (Research Institute, International Medical Center of Japan, Tokyo, Japan) for help and discussion. We also thank A Ryu, S Maki, and M Nagamoto for assistance and Y Kobayashi and T Fukui for discussion.

This work was supported in part by Grants-in-Aid (MEXT, Japan) B2 and S2, Takeda Medical Research Foundation, Smoking Research Foundation, Lilly Research Foundation, Research on Measures for Intractable Diseases (Health and Labor Science Research Grant), Special Coordination Funds for Promoting Science and Technology (JST), Research Grant of National Cardiovascular Center, Sankyo Research Foundation, the Korea Research Foundation Grant (KRF-2008-005-J00203), and the National Research Laboratory Program (ROA-2004-000-10359-0) funded by the Korean Government.

## References

[1] Engeli S. Role of the renin-angiotensin-aldosterone system in the metabolic syndrome. Contrib Nephrol 2006;151:122-34.
[2] Rahmouni K, Correia ML, Haynes WG, Mark AL. Obesity-associated hypertension: new insights into mechanisms. Hypertension 2005;45: 9-14.
[3] Dzau VJ. Circulating versus local renin-angiotensin system in cardiovascular homeostasis. Circulation 1988;77(6 Pt 2):I4-I13.
[4] Raizada V, Skipper B, Luo W, Griffith J. Intracardiac and intrarenal renin-angiotensin systems: mechanisms of cardiovascular and renal effects. J Investig Med 2007;55:341-59.

[5] Cassis LA, Saye J, Peach MJ. Location and regulation of rat angiotensinogen messenger RNA. Hypertension 1988;11(6 Pt 2): 591-6.

[6] Giacchetti G, Faloia E, Mariniello B, Sardu C, Gatti C, Camilloni MA, et al. Overexpression of the renin-angiotensin system in human visceral adipose tissue in normal and overweight subjects. Am J Hypertens 2002;15:381-8.

[7] Engeli S, Negrel R, Sharma AM. Physiology and pathophysiology of the adipose tissue renin-angiotensin system. Hypertension 2000;35: 1270-7.

[8] Massiera F, Seydoux J, Geloen A, Quignard-Boulange A, Turban S, Saint-Marc P, et al. Angiotensinogen-deficient mice exhibit impairment of diet-induced weight gain with alteration in adipose tissue development and increased locomotor activity. Endocrinology 2001; 142:5220-5.

[9] Massiera F, Bloch-Faure M, Ceiler D, Murakami K, Fukamizu A, Gasc JM, et al. Adipose angiotensinogen is involved in adipose tissue growth and blood pressure regulation. FASEB J 2001;15:2727-9.

[10] Frederich Jr RC, Kahn BB, Peach MJ, Flier JS. Tissue-specific nutritional regulation of angiotensinogen in adipose tissue. Hypertension 1992;19:339-44.

[11] Boustany CM, Bharadwaj K, Daugherty A, Brown DR, Randall DC, Cassis LA. Activation of the systemic and adipose renin-angiotensin system in rats with diet-induced obesity and hypertension. Am J Physiol Regul Integr Comp Physiol 2004;287:R943-9.

[12] Van Harmelen V, Ariapart P, Hoffstedt J, Lundkvist I, Bringman S, Arner P. Increased adipose angiotensinogen gene expression in human obesity. Obes Res 2000;8:337-41.

[13] Engeli S, Bohnke J, Gorzelniak K, Janke J, Schling P, Bader M, et al. Weight loss and the renin-angiotensin-aldosterone system. Hypertension 2005;45:356-62.

[14] Engeli S, Schling P, Gorzelniak K, Boschmann M, Janke J, Ailhaud G, et al. The adipose-tissue renin-angiotensin-aldosterone system: role in the metabolic syndrome? Int J Biochem Cell Biol 2003;35:807-25.

[15] Keaney Jr JF, Larson MG, Vasan RS, Wilson PW, Lipinska I, Corey D, et al. Obesity and systemic oxidative stress: clinical correlates of oxidative stress in the Framingham Study. Arterioscler Thromb Vasc Biol 2003;23:434-9.

[16] Urakawa H, Katsuki A, Sumida Y, Gabazza EC, Murashima S, Morioka K, et al. Oxidative stress is associated with adiposity and insulin resistance in men. J Clin Endocrinol Metab 2003;88:4673-6.

[17] Furukawa S, Fujita T, Shimabukuro M, Iwaki M, Yamada Y, Nakajima Y, et al. Increased oxidative stress in obesity and its impact on metabolic syndrome. J Clin Invest 2004;114:1752-61.

[18] Stocker R, Keaney Jr JF. Role of oxidative modifications in atherosclerosis. Physiol Rev 2004;84:1381-478.

[19] Grattagliano I, Palmieri VO, Portincasa P, Moschetta A, Palasciano G. Oxidative stress–induced risk factors associated with the metabolic syndrome: a unifying hypothesis. J Nutr Biochem 2008;19:491-504.

[20] Griendling KK, Minieri CA, Ollerenshaw JD, Alexander RW. Angiotensin II stimulates NADH and NADPH oxidase activity in cultured vascular smooth muscle cells. Circ Res 1994;74:1141-8.

[21] Das DK, Maulik N, Engelman RM. Redox regulation of angiotensin II signaling in the heart. J Cell Mol Med 2004;8:144-52.

[22] Sachse A, Wolf G. Angiotensin II–induced reactive oxygen species and the kidney. J Am Soc Nephrol 2007;18:2439-46.

[23] Brasier AR, Jamaluddin M, Han Y, Patterson C, Runge MS. Angiotensin II induces gene transcription through cell-type–dependent effects on the nuclear factor–kappaB (NF-kappaB) transcription factor. Mol Cell Biochem 2000;212:155-69.

[24] Hsieh TJ, Zhang SL, Filep JG, Tang SS, Ingelfinger JR, Chan JS. High glucose stimulates angiotensinogen gene expression via reactive oxygen species generation in rat kidney proximal tubular cells. Endocrinology 2002;143:2975-85.

[25] Brezniceanu ML, Liu F, Wei CC, Tran S, Sachetelli S, Zhang SL, et al. Catalase overexpression attenuates angiotensinogen expression and apoptosis in diabetic mice. Kidney Int 2007;71:912-23.

[26] Miyata K, Ohashi N, Suzaki Y, Katsurada A, Kobori H. Sequential activation of the reactive oxygen species/angiotensinogen/renin-angiotensin system axis in renal injury of type 2 diabetic rats. Clin Exp Pharmacol Physiol 2008;35:922-7.

[27] Houstis N, Rosen ED, Lander ES. Reactive oxygen species have a causal role in multiple forms of insulin resistance. Nature 2006;440:944-8.

[28] Frost SC, Lane MD. Evidence for the involvement of vicinal sulfhydryl groups in insulin-activated hexose transport by 3T3-L1 adipocytes. J Biol Chem 1985;260:2646-52.

[29] Fujimoto M, Masuzaki H, Tanaka T, Yasue S, Tomita T, Okazawa K, et al. An angiotensin II AT1 receptor antagonist, telmisartan augments glucose uptake and GLUT4 protein expression in 3T3-L1 adipocytes. FEBS Lett 2004;576:492-7.

[30] Sakai T, Sakaue H, Nakamura T, Okada M, Matsuki Y, Watanabe E, et al. Skp2 controls adipocyte proliferation during the development of obesity. J Biol Chem 2007;282:2038-46.

[31] Kobori H, Katsurada A, Miyata K, Ohashi N, Satou R, Saito T, et al. Determination of plasma and urinary angiotensinogen levels in rodents by newly developed ELISA. Am J Physiol Renal Physiol 2008;294: F1257-63.

[32] Oliveira HR, Verlengia R, Carvalho CR, Britto LR, Curi R, Carpinelli AR. Pancreatic beta-cells express phagocyte-like NAD(P)H oxidase. Diabetes 2003;52:1457-63.

[33] Saye JA, Cassis LA, Sturgill TW, Lynch KR, Peach MJ. Angiotensinogen gene expression in 3T3-L1 cells. Am J Physiol 1989;256(2 Pt 1): C448-51.

[34] Wajant H, Pfizenmaier K, Scheurich P. Tumor necrosis factor signaling. Cell Death Differ 2003;10:45-65.

[35] Cawthorn WP, Sethi JK. TNF-alpha and adipocyte biology. FEBS Lett 2008;582:117-31.

[36] Kamigaki M, Sakaue S, Tsujino I, Ohira H, Ikeda D, Itoh N, et al. Oxidative stress provokes atherogenic changes in adipokine gene expression in 3T3-L1 adipocytes. Biochem Biophys Res Commun 2006;339:624-32.

[37] Lee H, Lee YJ, Choi H, Ko EH, Kim JW. Reactive oxygen species facilitate adipocyte differentiation by accelerating mitotic clonal expansion. J Biol Chem 2009;284:10601-9.

[38] Lee YS, Kim AY, Choi JW, Kim M, Yasue S, Son HJ, et al. Dysregulation of adipose glutathione peroxidase 3 in obesity contributes to local and systemic oxidative stress. Mol Endocrinol 2008;22:2176-89.

[39] Wang B, Jenkins JR, Trayhurn P. Expression and secretion of inflammation-related adipokines by human adipocytes differentiated in culture: integrated response to TNF-alpha. Am J Physiol Endocrinol Metab 2005;288:E731-40.

[40] Jones BH, Standridge MK, Taylor JW, Moustaid N. Angiotensinogen gene expression in adipose tissue: analysis of obese models and hormonal and nutritional control. Am J Physiol 1997;273(1 Pt 2): R236-42.

[41] Aubert J, Safonova I, Negrel R, Ailhaud G. Insulin down-regulates angiotensinogen gene expression and angiotensinogen secretion in cultured adipose cells. Biochem Biophys Res Commun 1998;250: 77-82.

[42] Harte A, McTernan P, Chetty R, Coppack S, Katz J, Smith S, et al. Insulin-mediated upregulation of the renin angiotensin system in human subcutaneous adipocytes is reduced by rosiglitazone. Circulation 2005;111:1954-61.

[43] Morgan L, Broughton Pipkin F, Kalsheker N. Angiotensinogen: molecular biology, biochemistry and physiology. Int J Biochem Cell Biol 1996;28:1211-22.

[44] Thatcher S, Yiannikouris F, Gupte M, Cassis L. The adipose renin-angiotensin system: role in cardiovascular disease. Mol Cell Endocrinol 2009;302:111-7.

[45] Nyui N, Tamura K, Yamaguchi S, Nakamaru M, Ishigami T, Yabana M, et al. Tissue angiotensinogen gene expression induced by lipopolysaccharide in hypertensive rats. Hypertension 1997;30: 859-67.

[46] Flesch M, Hoper A, Dell'Italia L, Evans K, Bond R, Peshock R, et al. Activation and functional significance of the renin-angiotensin system in mice with cardiac restricted overexpression of tumor necrosis factor. Circulation 2003;108:598-604.
[47] Ron D, Brasier AR, Habener JF. Transcriptional regulation of hepatic angiotensinogen gene expression by the acute-phase response. Mol Cell Endocrinol 1990;74:C97-C104.
[48] Hotamisligil GS, Arner P, Caro JF, Atkinson RL, Spiegelman BM. Increased adipose tissue expression of tumor necrosis factor–alpha in human obesity and insulin resistance. J Clin Invest 1995;95: 2409-15.
[49] Xu H, Barnes GT, Yang Q, Tan G, Yang D, Chou CJ, et al. Chronic inflammation in fat plays a crucial role in the development of obesity-related insulin resistance. J Clin Invest 2003;112:1821-30.
[50] Ron D, Brasier AR, McGehee Jr RE, Habener JF. Tumor necrosis factor–induced reversal of adipocytic phenotype of 3T3-L1 cells is preceded by a loss of nuclear CCAAT/enhancer binding protein (C/EBP). J Clin Invest 1992;89:223-33.

*Am J Physiol Endocrinol Metab* 298: E930–E940, 2010.
First published September 23, 2009; doi:10.1152/ajpendo.00320.2009.

# Glucocorticoid reamplification within cells intensifies NF-κB and MAPK signaling and reinforces inflammation in activated preadipocytes

**Takako Ishii-Yonemoto, Hiroaki Masuzaki, Shintaro Yasue, Sadanori Okada, Chisayo Kozuka, Tomohiro Tanaka, Michio Noguchi, Tsutomu Tomita, Junji Fujikura, Yuji Yamamoto, Ken Ebihara, Kiminori Hosoda, and Kazuwa Nakao**

*Division of Endocrinology and Metabolism, Department of Medicine and Clinical Science, Kyoto University Graduate School of Medicine, Sakyoku, Japan*

Submitted 18 May 2009; accepted in final form 16 September 2009

**Ishii-Yonemoto T, Masuzaki H, Yasue S, Okada S, Kozuka C, Tanaka T, Noguchi M, Tomita T, Fujikura J, Yamamoto Y, Ebihara K, Hosoda K, Nakao K.** Glucocorticoid reamplification within cells intensifies NF-κB and MAPK signaling and reinforces inflammation in activated preadipocytes. *Am J Physiol Endocrinol Metab* 298: E930–E940, 2010. First published September 23, 2009; doi:10.1152/ajpendo.00320.2009.—Increased expression and activity of the intracellular glucocorticoid-reactivating enzyme 11β-hydroxysteroid dehydrogenase type 1 (11β-HSD1) contribute to dysfunction of adipose tissue. Although the pathophysiological role of 11β-HSD1 in mature adipocytes has long been investigated, its potential role in preadipocytes still remains obscure. The present study demonstrates that the expression of 11β-HSD1 in preadipocyte-rich stromal vascular fraction (SVF) cells in fat depots from *ob/ob* and diet-induced obese mice was markedly elevated compared with lean control. In 3T3-L1 preadipocytes, the level of mRNA and reductase activity of 11β-HSD1 was augmented by TNF-α, IL-1β, and LPS, with a concomitant increase in inducible nitric oxide synthase (iNOS), monocyte chemoattractant protein-1 (MCP-1), or IL-6 secretion. Pharmacological inhibition of 11β-HSD1 and RNA interference against 11β-HSD1 reduced the mRNA and protein levels of iNOS, MCP-1, and IL-6. In contrast, overexpression of 11β-HSD1 further augmented TNF-α-induced iNOS, IL-6, and MCP-1 expression. Moreover, 11β-HSD1 inhibitors attenuated TNF-α-induced phosphorylation of NF-κB p65 and p38-, JNK-, and ERK1/2-MAPK. Collectively, the present study provides novel evidence that inflammatory stimuli-induced 11β-HSD1 in activated preadipocytes intensifies NF-κB and MAPK signaling pathways and results in further induction of proinflammatory molecules. Not limited to 3T3-L1 preadipocytes, we also demonstrated that the notion was reproducible in the primary SVF cells from obese mice. These findings highlight an unexpected, proinflammatory role of reamplified glucocorticoids within preadipocytes in obese adipose tissue.

11β-hydroxysteroid dehydrogenase type 1; preadipocyte; nuclear factor-κB; mitogen-activated protein kinase; adipose inflammation

OBESE ADIPOSE TISSUE IS CHARACTERIZED by low-grade, chronic inflammation (24, 58). In humans and rodents, it has been shown that intracellular glucocorticoid reactivation is exaggerated in obese adipose tissue (38). Two isoenzymes, 11β-hydroxysteroid dehydrogenase type 1 (11β-HSD1) and type 2 (11β-HSD2), catalyze interconversion between hormonally active cortisol and inactive cortisone (2). In particular, 11β-HSD1 is abundantly expressed in adipose tissue and preferentially reactivates cortisol from cortisone (2). In contrast, 11β-HSD2 inactivates cortisol mainly in tissues involved in water and electrolyte metabolism (60). Transgenic mice overexpressing 11β-HSD1 in adipose tissue display a cluster of fuel dyshomeostasis (61). Conversely, systemic 11β-HSD1 knockouts and adipose-specific 11β-HSD2 overexpressors, which mimic adipose-specific 11β-HSD1 knockouts, are completely protected against diabetes and dyslipidemia on a high-fat diet (14, 30, 31, 42). Interestingly, 11β-HSD1 knockout mice on a high-fat diet showed preferential accumulation of subcutaneous adipose tissue, whereas wild-type mice accumulated considerable fat pads also in visceral (mesenteric) adipose tissue (39). These findings suggest that increased activity of 11β-HSD1 in adipose tissue contributes to dysfunction of adipose tissue and subsequent metabolic derangement.

Adipose tissue is composed of mature adipocytes (~50–70% of total cells), preadipocytes (~20–40%), macrophages (~1–30%), and other cell types (22). Biopsy studies of human adipose tissue demonstrated that the distribution of adipocyte diameter is bimodal, consisting of populations of very small adipocytes ("differentiating preadipocytes") and mature adipocytes (28, 35). Interestingly, the proportion of very small adipocytes was higher in obese people compared with the lean controls (28). Notably, insulin resistance was associated with an expanded population of small adipocytes and decreased expression of differentiation marker genes, suggesting that impairment of adipocyte differentiation may contribute to obesity-associated insulin resistance (35). In this context, a potential link between preadipocyte function and pathophysiology of obese adipose tissue has recently attracted research interest (53, 57).

Many of the genes overexpressed in mature adipocytes are associated with metabolic and secretory function, whereas the most representative function of the genes overexpressed in nonmature adipocytes, i.e., stromal vascular fraction (SVF) cells, is related to inflammation and immune response (9). Macrophage infiltration into obese adipose tissue contributes to local and systemic inflammation in subjects with obesity (63, 65). Furthermore, recent research (12, 48) highlights a pathophysiological role of preadipocytes in obese adipose tissue. In the proinflammatory milieu, preadipocytes act as macrophages (11, 13), share in phagocytic activities (11), and secrete an array of inflammatory substances (13).

A pharmacological dose of glucocorticoids is widely used for anti-inflammatory therapies in human clinics (49). On the other hand, recent research is highlighting the stimulatory effects of glucocorticoids on inflammatory response. Such effects are observed at lower concentrations relevant to phys-

Address for reprint requests and other correspondence: H. Masuzaki, Division of Endocrinology and Metabolism, Dept. of Medicine and Clinical Science, Kyoto University Graduate School of Medicine, 54, Shogoin Kawaharacho, Sakyoku, Kyoto, 606-8507, Japan (e-mail: hiroaki@kuhp.kyoto-u.ac.jp).

iological stress in vivo (35, 55, 66). Therefore, the potential role of 11β-HSD1 in a variety of inflammatory responses has stimulated academic interest (10, 26). Furthermore, it is known that mature adipocytes abundantly express 11β-HSD1, which is related to adipocyte dysfunction in obese adipose tissue (44, 61). On the other hand, the role of 11β-HSD1 in SVF cells remains largely unclear.

In this context, the present study was designed to explore the expression, regulation, and pathophysiological role of 11β-HSD1 in activated preadipocytes. The results demonstrate that inflammatory stimuli-induced 11β-HSD1 reinforces NF-κB and MAPK signals and results in induction of proinflammatory molecules.

## MATERIALS AND METHODS

*Reagents and chemicals.* All reagents were of analytical grade unless otherwise indicated. TNF-α, IL-1β, LPS, and carbenoxolone (3, 52), a nonselective inhibitor for 11β-HSD1 and 11β-HSD2, were obtained from Sigma-Aldrich (St. Louis, MO). The recently developed 11β-HSD1 selective inhibitors 3-(1-adamantyl)-5,6,7,8,9,10-hexahydro[1,2,4]triazolo[4,3-α]azocine trifluoroacetate salt (WO03/065983, inhibitor A; Merck, Whitehouse Station, NJ; Ref. 23) and 2,4,6-trichloro-*N*-(5,5-dimethyl-7-oxo-4,5,6,7-tetrahydro-1,3-benzothiazol-2-yl) benzenesulfonamide (BVT-3498; Biovitrum, Stockholm, Sweden; Ref. 25) were synthesized according to the patent information.

Polyclonal antibodies against NF-κB p65, phospho-p65, p38 MAPK, phospho-p38, ERK1/2, phospho-ERK1/2, JNK, phospho-JNK, Akt, and phospho-Akt were purchased from Cell Signaling Technology (Beverly, MA). Polyclonal antibodies against SHIP1, PP2A, and MKP-1 were purchased from Santa Cruz Biotechnology (Santa Cruz, CA). An antibody against β-actin was purchased from Upstate Biotechnology (Lake Placid, NY). Horseradish peroxidase-conjugated anti-mouse, anti-rat, and anti-rabbit IgG antibodies and ECL Plus Western blotting detection kits were purchased from Amersham Biosciences (Piscataway, NJ).

*Cell culture.* 3T3-L1 cells (kindly provided by Dr. H. Green and Dr. M. Morikawa, Harvard Medical School, Boston, MA) were maintained in DMEM containing 10% (vol/vol) calf serum at 37°C under 10% $CO_2$.

*Animals.* Seventeen-week-old male C57BL/6 and nine-week-old *ob/ob* mice were used for the experiments. Mice were maintained on a standard diet (F-2, 3.7 kcal/g, 12% of kcal from fat, source soybean; Funahashi Farm) or a high-fat diet (Research Diets D12493, 5.2 kcal/g, 60% of kcal from fat, source soybean/lard) under a 14:10-h light-dark cycle at 23°C. The high-fat diet was administered to the diet-induced obese (DIO) mice from 3 to 17 wk of age. Animals were allowed free access to food and water. All animal experiments were undertaken in accordance with the guidelines for animal experiments of the Kyoto University Animal Research Committee.

*Isolation of SVF and the mature adipocyte fraction.* Subcutaneous (SQ), mesenteric (Mes), and epididymal (Epi) fat deposits were chopped using fine scissors and digested with 2 mg/ml collagenase (Type VIII; Sigma-Aldrich) in DMEM for 1 h at 37°C under continuous shaking (170 rpm). Dispersed tissue was filtered through a nylon mesh with a pore size of 250 μm and centrifuged. Digested material was separated by centrifugation at 1,800 rpm for 5 min. The sedimented SVF and cell supernatant [mature adipocyte fraction (MAF)] were both washed with DMEM. For primary culture experiments, SVF cells from epididymal fat pads were plated in sixwell plates and cultured overnight in DMEM containing 10% (vol/vol) FBS at 37°C under 10% $CO_2$. After being rinsed with the medium three times, the cells were incubated with or without TNF-α, carbenoxolone, or inhibitor A for 24 h.

*Quantitative real-time PCR.* Total RNA was extracted using Trizol reagent (Invitrogen, Carlsbad, CA), and cDNA was synthesized using an iScript cDNA synthesis kit (Bio-Rad, Hercules, CA) according to the manufacturer's instruction. The sequences of probes and primers are summarized in Suppl. Table S1 (supplemental data for this article are available at the *Am J Physiol Endocrinol Metab* website). Taqman PCR was performed using an ABI Prism 7300 sequence detection system following the manufacturer's instructions (Applied Biosystems, Foster City, CA). mRNA levels were normalized to those of 18S rRNA.

*11β-HSD1 enzyme activity assay.* 11β-HSD1 acts as a reductase and reactivates cortisol from cortisone in viable cells (54). In certain substrates, however, such as tissue homogenates or the microsome fraction, 11β-HSD1 acts as a dehydrogenase and inactivates cortisol to cortisone (8). 11β-HSD1 reductase activity in intact cells was measured as reported previously (8). Cells were incubated for 24 h in serum-free DMEM, with the addition of 250 nM cortisone and tritium-labeled tracer $[1,2\text{-}^3H]_2$-cortisone (Muromachi Yakuhin, Kyoto, Japan) for reductase activity and 250 nM cortisol with $[1,2,6,7\text{-}^3H]_4$-cortisol (Muromachi Yakuhin) for dehydrogenase activity. Cortisol and cortisone were extracted using ethyl acetate, evaporated, resuspended in ethanol, separated using thin-layer chromatography in 95:5 chloroform/methanol, and quantified using autoradiography.

To validate inhibitory potency of compounds against 11β-HSD1 with the use of FreeStyle 293 cells transiently transfected with human 11β-HSD1, the enzyme activity assay was carried out with 20 mM Tris · HCl at pH 7.0, 50 μM NADPH, 5 μg protein of microsomal fraction, and 300 nM [$^3$H]cortisone for 2 h. The reaction was stopped by 18β-glycyrrhetinic acid. The labeled cortisol product was captured by mouse monoclonal anti-cortisol antibody, bound to scintillation proximity assay beads coated with protein A, and quantified in a scintillation counter.

*ELISA.* Monocyte chemoattractant protein-1 (MCP-1) and IL-6 concentrations in the cultured media of 3T3-L1 preadipocytes were measured using ELISA according to the manufacturer's instructions (R&D Systems, Minneapolis, MN).

*Western blot analysis.* Two days after confluence, 3T3-L1 preadipocytes were stimulated with 10 ng/ml TNF-α in the absence or presence of 11β-HSD1 inhibitors (50 μM carbenoxolone or 10 μM inhibitor A) for 24 h.

For primary culture experiments, SVF from epididymal fat pads were plated in sixwell plates and cultured overnight in DMEM containing 10% (vol/vol) FBS at 37°C under 10% $CO_2$. After being rinsed with the medium three times, the cells were incubated with or without TNF-α, carbenoxolone, or inhibitor A for 24 h.

After 2-h serum starvation, cells were treated with TNF-α for 10 min to detect NF-κB and MAPK signals. Cells were washed with ice-cold PBS and harvested in lysis buffer (1% wt/vol SDS, 60 mM Tris · HCl, 1 mM $Na_3VO_4$, 0.1 mg/ml aprotinin, 1 mM PMSF, and 50 nM okadaic acid at pH 6.8) and boiled at 100°C for 10 min. After centrifugation, supernatants were normalized to the protein concentration via the Bradford method and then equal amounts of protein were subjected to SDS-PAGE and immunoblot analysis.

*RNA interference.* We tested four different small interfering RNA (siRNA) sequences. Stealth RNAi for mouse 11β-HSD1 (MSS205244, MSS205245, and MSS205246) (Invitrogen), and RNA interference (RNAi) for mouse 11β-HSD1 originally designed by an siRNA Design Support System (TaKaRa Bio, Shiga, Japan; sense: 5′-GAAAUGGCAUAUCAUCUGUTT-3′ and antisense: 3′-TTCUUUACCGUAUAGUAGACA-5′). MSS205245 and MSS205246 did not suppress the 11β-HSD1 mRNA level effectively in preliminary experiments. Therefore, we demonstrated the data of MSS205244 [si(1)] and of the originally designed siRNA [si(2)] in this study. According to the manufacturer's protocol, 3T3-L1 preadipocytes were transfected with 10 nM siRNA in antibiotic-free medium using Lipofectamine RNAiMAX (Invitrogen). We assessed the ransfection efficiency using green fluorescent protein (GFP) detection (pmaxGFP), according to the manufacturer's instructions (Amaxa, Cologne, Germany). Fluorescent microscopic observa-

tion revealed that more than two-thirds of the cells expressed GFP (data not shown).

*Expression vector.* A mammalian expression vector encoding Hsd11b1 (Hsd11b1/pcDNA3.1) was constructed by inserting cDNA for mouse 11β-HSD1 into pcDNA3.1 (Invitrogen). 3T3-L1 preadipocytes were detached from culture dishes using 0.25% trypsin. Cells ($5 \times 10^6$) were mixed with 2 μg plasmid in the solution provided with the cell line Nucleofector Kit V (Amaxa). pcDNA3.1/11β-HSD1 or a control vector was introduced into the cells using electroporation with a Nucleofector (Amaxa) instrument according to the manufacturer's instructions.

*Statistical analysis.* Data are expressed as the means ± SE of triplicate experiments. Data were analyzed using one-way ANOVA, followed by Student's *t*-tests for each pair of multiple comparisons. Differences were considered significant if $P < 0.05$.

## RESULTS

*Expression of 11β-HSD1 was elevated in the MAF and in SVF isolated from fat depots in ob/ob mice and DIO mice.* Genetic (*ob/ob*) and dietary (DIO) obese models were analyzed. Expression of iNOS, MCP-1, and IL-6, all of which are obesity-related proinflammatory mediators (19, 29, 45, 56), was elevated in the MAF and SVF from both *ob/ob* mice and DIO mice compared with lean littermates (Fig. 1, *A* and *B*). Levels of 11β-HSD1 mRNA in the MAF from obese mice were substantially elevated compared with their lean littermates (*ob/ob*: SQ, 5-fold; Mes, 62-fold) (DIO: SQ, 24-fold; Mes, 460-fold; Fig. 1, *A* and *B*). On the other hand, levels of 11β-HSD1 mRNA in SVF from *ob/ob* mice and DIO mice were also elevated compared with their lean littermates (*ob/ob*: SQ, 3-fold; Mes, 3-fold; and DIO: SQ, 8-fold, Mes, 4-fold; Fig. 1, *A* and *B*).

*TNF-α, IL-1β, and LPS augmented 11β-HSD1 mRNA expression and reductase activity in 3T3-L1 preadipocytes.* When 3T3-L1 preadipocytes were treated with TNF-α (10 ng/ml) for 24 h, mRNA levels of 11β-HSD1 markedly increased (~4-fold; Fig. 2*iv*). Levels of iNOS, MCP-1, and IL-6 mRNA were concomitantly increased (50-, 70-, and 200-fold, respectively; Fig. 2, *i–iii*). IL-1β (1 ng/ml) and LPS (1,000 ng/ml) substantially augmented 11β-HSD1 mRNA expression in 3T3-L1 preadipocytes (10- and 3-fold vs. control, respectively) (Fig. 2*iv*). Reductase activity of 11β-HSD1 was augmented by TNF-α, IL-1β, and LPS compared with the control (2-, 9-, and 6-fold vs. control, respectively; $P < 0.05$; Fig. 2*v*). Based on the results of 11β-HSD1 activity, TNF-α was used at 10 ng/ml in subsequent experiments. On the other hand, 11β-HSD2 mRNA and the corresponding dehydrogenase activity were undetected not only at the baseline condition but with TNF-α, IL-1β, and LPS treatments (data not shown).

*Dexamethasone decreased iNOS, MCP-1, and IL-6 mRNA and protein levels in TNF-α-treated 3T3-L1 preadipocytes.* The effects of glucocorticoid on proinflammatory gene expression in TNF-α-treated 3T3-L1 preadipocytes were examined over a wide range of concentrations ($10^{-10}$, $10^{-9}$, $10^{-8}$, and $10^{-7}$ M), representing physiological to therapeutical levels in vivo (5). Dexamethasone ($10^{-7}$ M) decreased mRNA levels of iNOS, MCP-1, and IL-6 (iNOS: 85 ± 2%, MCP-1: 40 ± 16%, and IL-6: 97 ± 1% reduction vs. TNF-α-treated cells) and protein levels in the media (MCP-1: 48 ± 5% and IL-6: 83 ± 1% reduction) in TNF-α-treated 3T3-L1 preadipocytes (Suppl. Fig. S1).

*Pharmacological inhibition of 11β-HSD1 attenuated iNOS, MCP-1, and IL-6 mRNA and protein levels in TNF-α-treated 3T3-L1 preadipocytes.* The effects of pharmacological inhibition of 11β-HSD1 on proinflammatory gene expression were examined in TNFα-treated 3T3-L1 preadipocytes. In previous in vitro studies, carbenoxolone (CBX), a nonselective inhibitor of 11β-HSD1 and 11β-HSD2, was used at concentrations from 5 to 300 μM (16, 17, 26). To date, an 11β-HSD1-specific

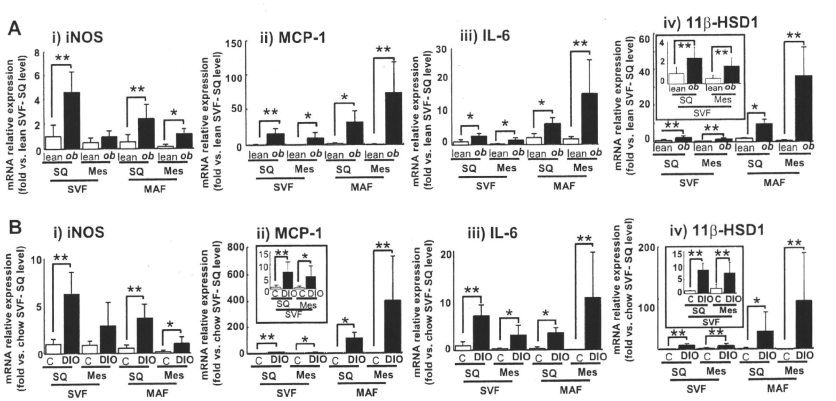


Fig. 1. 11β-Hydroxysteroid dehydrogenase type 1 (11β-HSD1) mRNA expression in stromal vascular fraction cells (SVF) and mature adipocytes fraction (MAF) isolated from obese adipose tissue of *ob/ob* mice and diet-induced obese (DIO) mice. *A*: *ob/ob* and lean littermates [control (C) 9 wk of age; $n = 6$]. *B*: DIO and littermates on a chow diet (17 wk of age; $n = 6$). Levels of inducible nitric oxide synthase (iNOS; *i*), monocyte chemoattractant protein-1 (MCP-1; *ii*), IL-6 (*iii*), and 11β-HSD1 (*iv*) mRNA in SVF and MAF in subcutaneous abdominal fat depots (SQ) and mesenteric fat depots (Mes). $^*P < 0.05$, $^{**}P < 0.01$ compared with lean littermates.

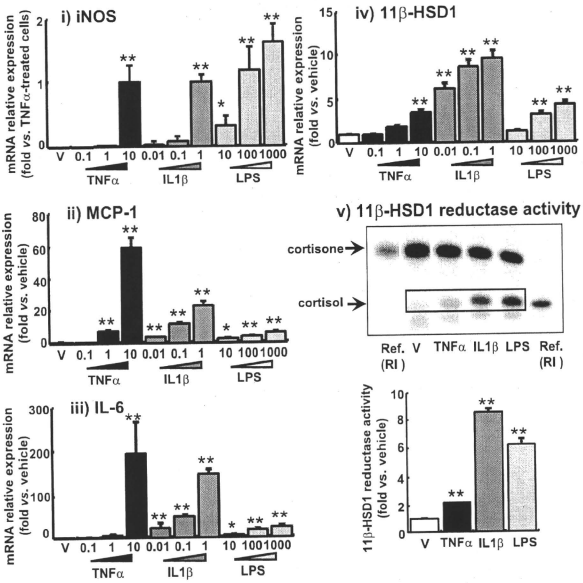


Fig. 2. TNF-α, IL-1β, and LPS augment the expression of proinflammatory mediators and 11β-HSD1 in 3T3-L1 preadipocytes. Cells were treated with TNF-α (0.1, 1, and 10 ng/ml), IL-1β, (0.01, 0.1, and 1 ng/ml) or LPS (10, 100, and 1,000 ng/ml) for 24 h. Levels of iNOS (*i*), MCP-1 (*ii*), IL-6 (*iii*), and 11β-HSD1 (*iv*) mRNA were quantified using real-time PCR. Values were normalized to that of 18S rRNA. *v*: 11β-HSD1 reductase activity (expressed as conversion ability of cortisone to cortisol) was assessed in the medium of 3T3-L1 cells treated with 10 ng/ml TNF-α, 1 ng/ml IL-1β, or 1,000 ng/ml LPS for 24 h. A reference of [$^3$H]cortisone or [$^3$H]cortisol was used as a size marker. A representative autoradiograph of thin-layer chromatography in 11β-HSD reductase activity assay (*top*) and quantification (*bottom*). Intensities of cortisol signals correspond to the enzyme activity of reductase. Ref. (RI), reference samples of [$^3$H]cortisone or [$^3$H]cortisol as size marker. Data are means ± SE of triplicate experiments. $^*P < 0.05$, $^{**}P < 0.01$, compared with vehicle (V)-treated group.

inhibitor, inhibitor A, has not been used for in vitro studies; however, another 11β-HSD1-specific inhibitor (compound 544) sharing almost the same structure as inhibitor A was used at a concentration of 5 μM (62). Therefore, in the present study, 10–50 μM CBX and 2.5–10 μM inhibitor A were used.

Before using these inhibitors in intact cells, we validated inhibitory potency of compounds against 11β-HSD1 in the microsome fraction assay. We verified that inhibitor A (10 nM) and CBX (1 μM) inhibited 11β-HSD1 activity as little as 25% vs. control, respectively, and that both of the 11β-HSD inhibitors suppressed 11β-HSD activity in a dose-dependent manner (Suppl. Fig. S2).

In 3T3-L1 preadipocytes, although CBX and inhibitor A did not change the level of 11β-HSD1 reductase activity, both of them suppressed TNF-α-induced reductase activity of 11β-HSD1 in a dose-dependent manner (Fig. 3*A*). CBX (50 μM) and inhibitor A (10 μM) markedly attenuated 11β-HSD1 activity (78 and 60% reduction vs. TNF-α-treated cells, respectively; Fig. 3*A*).

Without TNF-α-treatment, CBX and inhibitor A did not affect mRNA or protein levels of iNOS, MCP-1, and IL-6. On the other hand, in TNF-α-treated cells, these inhibitors reduced the mRNA and protein levels of proinflammatory genes. CBX decreased iNOS, MCP-1, and IL-6 mRNA levels (50 μM; iNOS: 83 ± 5%, MCP-1: 27 ± 4%, and IL-6: 47 ± 10% reduction vs. TNF-α-treated cells without compounds) and protein levels in the media (MCP-1: 17 ± 1% and IL-6: 34 ± 6% reduction) in TNF-α-treated 3T3-L1 preadipocytes (Fig. 3*B*). Similarly, inhibitor A reduced iNOS, MCP-1, and IL-6 mRNA (10 μM; iNOS: 47 ± 13%, MCP-1: 32 ± 12%, and IL-6: 33 ± 9% reduction) and protein levels in the media (MCP-1: 47 ± 3% and IL-6: 14 ± 3% reduction) (Fig. 3*C*).

*Effect of 11β-HSD1 knockdown on proinflammatory properties in 3T3-L1 preadipocytes.* To explore the potential role of 11β-HSD1 in cytokine release from activated preadipocytes, 11β-HSD1 was knocked down using siRNA. We tested four different siRNA sequences as described in MATERIALS AND METHODS; however, two of them did not suppress 11β-HSD1 mRNA level significantly in the preliminary experiments. Thus we demonstrated the data on si(1) and si(2).

When 3T3-L1 preadipocytes were transfected with 11β-HSD1 siRNA, TNF-α-induced expression of 11β-HSD1 was markedly attenuated [si(1): 60 ± 9% and si(2): 88 ± 7% reduction vs. negative control siRNA; Fig. 4*A*, *i*]. 11β-HSD1 reductase activity was also decreased by 11β-HSD1 siRNA [si(1): 81 ± 9% and si(2): 84 ± 3% reduction vs. negative control siRNA; Fig. 4*A*, *ii*]. 11β-HSD2 mRNA levels and the corresponding dehydrogenase activity were under detectable with or without siRNA treatments in 3T3-L1 preadipocytes (data not sown). Negative control RNAi did not influence the expression of 11β-HSD1. Knockdown of 11β-HSD1 in TNF-α-treated 3T3-L1 preadipocytes effectively reduced iNOS, MCP-1, and IL-6 mRNA levels [si(1): IL-6: 32 ± 7% reduction; and si(2): iNOS: 37 ± 8%, MCP-1: 22 ± 5%, and IL-6: 59 ± 3% reduction] and protein levels in the media [si(1):

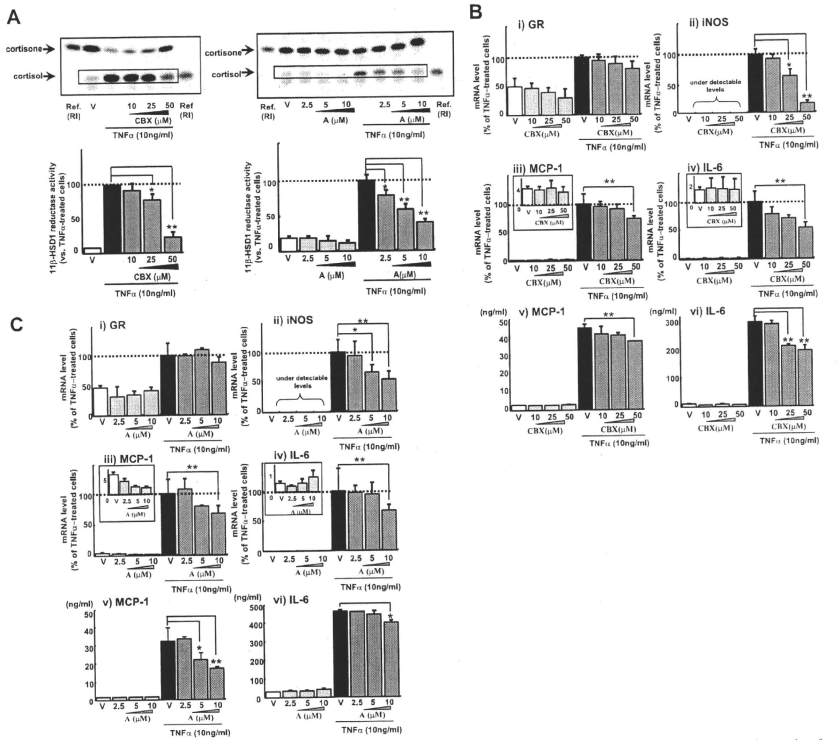


Fig. 3. Effects of pharmacological inhibition of 11β-HSD1 on glucocorticoid receptor (GR), MCP-1, IL-6, and iNOS expression in and secretion from TNF-α-treated 3T3-L1 preadipocytes. *A*: 11β-HSD1 activity assay for validation of 11β-HSD1 inhibitors. 3T3-L1 preadipocytes were incubated for 24 h in serum-free DMEM, adding 250 nM of cortisone with tritium-labeled cortisone. A representative autoradiograph of TLC for the 11β-HSD1 activity assay (*top*) and quantification of 11β-HSD1 activities (*bottom*). Intensities of cortisol signals correspond to the reductase activity. The *y*-axis shows percent 11β-HSD1 reductase activity compared with TNF-α (10 mg/ml)-treated cells. carbenoxolone (CBX; 10–50 μM) and inhibitor A (A; 2.5–10 μM) substantially reduced 11β-HSD1 activity in 3T3-L1 preadipocytes. CBX (*B*; 10–50 μM) and inhibitor A (*C*; 2.5–10 μM) 3T3-L1 preadipocytes were treated with TNF-α (10 ng/ml) or cotreated with CBX and inhibitor A for 24 h. GR (*i*), iNOS (*ii*), MCP-1 (*iii*), and IL-6 (*iv*) mRNA levels were determined using real-time PCR. Values were normalized to that of 18S rRNA and expressed relative to TNF-α-treated cells. Concentrations of MCP-1 (*v*) and IL-6 (*vi*) in the medium were measured with ELISA. Data are means ± SE of triplicate experiments. $*P < 0.05$, $** P < 0.01$, compared with TNF-α-treated cells.

MCP-1: 13 ± 1% and IL-6: 17 ± 1% reduction; and si(2): MCP1: 19 ± 7% and IL-6: 30 ± 1% reduction; Fig. 4*B*].

*Overexpression of 11β-HSD1 augmented iNOS, MCP-1, and IL-6 in TNF-α-treated 3T3-L1 preadipocytes.* We examined whether overexpression of 11β-HSD1 is relevant to the augmentation of proinflammatory molecules in activated preadipocytes. The extent of 11β-HSD1 overexpression in 3T3-L1 preadipocytes was assessed by 11β-HSD1 mRNA levels and reductase activity (Fig. 5*A*). As expected, 11β-HSD1 mRNA level was increased by treatment of the 11β-HSD1 vector (~20-fold) or 10 ng/ml TNF-α (~300-fold) compared with the vehicle. TNF-α-induced expression of 11β-HSD1 was further augmented by the introduction of the 11β-HSD1 vector (1.6-fold vs. empty vector). Reductase activity of 11β-HSD1 was also increased by the introduction of the vector (2-fold) or 10 ng/ml TNF-α (10-fold). Notably, TNF-α-induced enzyme activity was further augmented by the vector (1.3-fold vs. empty vector).

Expression of iNOS, MCP-1, and IL-6 did not differ between the 11β-HSD1 vector and the empty vector. On the other hand, TNF-α-induced expression of iNOS, MCP-1, and IL-6 was augmented in 11β-HSD1 transfectants (MCP-1: 172 ±